Ground-state properties of a single oxygen hole in a CuO_2 plane

D. M. Frenkel* and R. J. Gooding†
Laboratory of Atomic and Solid State Physics, Cornell University, Ithaca, New York 14853-2501

B. I. Shraiman
AT&T Bell Laboratories, Murray Hill, New Jersey 07974

E. D. Siggia
Laboratory of Atomic and Solid State Physics, Cornell University, Ithaca, New York 14853-2501
and Ecole Normale Superieure, 24 Rue Lhomond, Paris, France
(Received 8 June 1989)

The properties of a single O hole, either localized or mobile, in a CuO_2 plane are studied for an effective Hamiltonian derived from the extended Hubbard model in the strong-coupling limit. The ground-state wave function for a 16-Cu-site cluster is found exactly and compared with a semiclassical variational treatment of the same problem. In the ground state, whether localized or mobile, there is a long-range dipolar distortion of the Cu spin background around the O hole, as well as a strong antiferromagnetic correlation between the spin of the O hole and the two adjacent Cu spins (corresponding to the "3-spin polaron"). These correlations are forced by hopping and/or direct Cu-O exchange and can be saturated by either one of them, suggesting that the two processes have similar effects on the spin configuration and do not significantly interfere. The minimum of the mobile hole band lies at $\mathbf{k}=(\pm\pi/2,\pm\pi/2)$ (at least in the presence of the small oxygen-oxygen hopping). The bandwidth scales with the Cu-Cu exchange and not the bare hopping, when the former is smaller. The ground state has spin $\frac{1}{2}$ with the z magnetization residing in the canting of the Cu spins, and the expectation value of the O spin vector being very nearly zero. Thus, both the quantum numbers of the mobile vacancy ground state, as well as the far-field structure of the Cu spin configuration, are the same as those found for the vacancy in the single-band t-J model.

I. INTRODUCTION

The ubiquitous structural feature of all of the Cu-based high-temperature superconductors[1] is the cuprous oxide plane, and the theoretical description of these planes has been intensely investigated.[2] Anderson[3] first suggested that the CuO_2 planes could be described by an effective single-band large-U Hubbard model, where only holes in the Cu d orbitals are considered. A more realistic model for these planes, proposed by Varma *et al.*,[4] and Emery,[5] is the extended two-band Hubbard model that explicitly accounts for both the Cu and O orbitals.

For the stoichiometric composition, both the single-band and two-band models describe antiferromagnetic (hereafter denoted by AF) insulators if the Coulombic repulsion between carriers is larger than their characteristic hopping frequency. It is now established[6] that La_2CuO_4 and $YBa_2Cu_3O_6$ are AF insulators, and magnetic form-factor measurements,[7] and an x-ray-absorption near-edge spectroscopy (XANES) study,[8] demonstrate that the spins form strongly localized Cu^{2+} configurations interacting via superexchange.[9] The only difference, in this case, between the two aforementioned models is in the expression of the superexchange constant.

The difference between a one- and two-band formulation of the CuO_2 plane becomes important when one considers (i) doping the stoichiometric AF insulator La_2CuO_4 with a divalent ion, such as Sr, or (ii) adding more oxygen to $YBa_2Cu_3O_6$. These modifications introduce hole carriers into the Cu-O planes, and there is strong experimental evidence[10] that the holes are predominantly on the O sites. Thus, in general, an extended two-band Hubbard model would be required to describe the behavior of the carriers. However, it has been suggested by Zhang and Rice[11] that in a certain limit of parameter values the two-band model can be formally reduced to a single-band model, as proposed by Anderson.[3]

It is technically advantageous to pass immediately to the strong-coupling limit[5,12–17] of the extended Hubbard model and project onto basis states in which each Cu site has a spin $\frac{1}{2}$, and the holes (also with spin $\frac{1}{2}$) are restricted to O sites. Virtual transitions then give rise to an AF exchange interaction between nearest-neighbor Cu sites, and between Cu sites and O holes,[18] as well as processes in which holes hop from O to O through the intervening Cu sites. The analogous reduction of the single-band Hubbard model leads to the so-called t-J Hamiltonian (hopping and exchange). In either case, however, because of the strong coupling between the hole and the surrounding Cu spins, the problem remains highly nontrivial even in the extreme dilution limit of a single O hole. Thus, as a prerequisite for better understanding the physics of doped Cu-O layers it is important to achieve a quantitative understanding of the ground state of a single

mobile hole. This problem has been addressed by a number of recent studies of both one-band (or t-J) model[19–28] and the two-band model.[13,15–17,29–32]

To motivate the present study we summarize several key points that emerged in the earlier work. First, for the t-J model in the interesting limit of $t \gg J$, one observes that while the hopping hole strongly modifies the local Cu spin environment, the translational symmetry guarantees that the states can be labeled by a Bloch index. However, in contrast with the free-carrier situation, the bottom of the band lies at the zone-face centers,[20–25] and the bandwidth scales as J, not t. In addition, the spins further removed from the hole display a coherent long-range distortion[22] with dipolar symmetry which is induced by the hopping of the hole and can be associated with the "backflow" of the magnetization current in the spin background. The presence of such a distortion and the implied coupling to the "twist" of the staggered magnetization order parameter has important implications for the AF long-range order in the presence of the finite density of holes.[33]

Curiously, for the two-band model, Aharony *et al.*[18] have pointed out a dipolar distortion of the Cu spin configuration arising from a very different process: For the hole localized on a given bond the direct Cu-O exchange tends to align the two neighboring Cu spins, forcing a distortion of the background. While the Aharony *et al.* argument was purely classical, it appears consistent with the presence of the quantum, "3-spin polaron" on the vacant (i.e., occupied by the hole) bond, as proposed by Emery and Reiter.[15] The important question, however, concerns the effect of hopping on this structure. On the other hand, the work of Roth[30] on the band structure of the O hole moving in the Néel ordered Cu spin background suggests that the bottom of the hole band lies at the magnetic zone boundary, but the analysis does not include the effects of spin exchange.

The competition of the hopping and exchange effects in the two-band model can be investigated numerically for small clusters. A study of this type has been initiated by Shiba and Ogata[13,29] who found the O hole ground state on the 10-Cu-site cluster. The motivation for the present study of the 16-Cu-site cluster is to obtain more conclusive results for the O hole band structure, compare the structure of the spin distortion due to the hopping and the one induced by the direct Cu-O exchange and, finally, compare the results to those for the t-J model.

The reduction of the two-Hubbard model to a model with effective hopping and exchange is useful since it at least doubles the cluster size that can be treated exactly. However, extracting useful information from the exact wave function is entirely nontrivial. The wave function is complicated since it describes the correlations amongst the total magnetization, the spin of the hole, the AF order parameter, various Cu spins, as well as the spatial symmetries. Hence, we explore a number of correlation functions, the choice of which is motivated by the semiclassical variational wave functions, to which we resort to gain insight.

The paper is organized as follows. In Sec. II we derive the effective Hamiltonian. In Sec. III we give our numerical results for small clusters, for both a quenched and mobile hole. In Sec. IV we develop the perturbation theory utilizing the semiclassical approximation, and present additional numerical results that further characterize the ground state, e.g., effective masses, and long-range behavior of the distortion pattern. In Sec. V we explore the consequences of adding a direct oxygen hopping term to our Hamiltonian. Section VI summarizes the relation of the quantum and semiclassical calculations, comments on the relation between the one and two-band models in the strong-coupling limit, and mentions the possible relevance of this work to experiments.

II. EFFECTIVE HAMILTONIAN

The extended Hubbard model[5] is given by

$$\hat{H}=\sum_{i,j,\sigma}\varepsilon_{ij}a_{i\sigma}^{\dagger}a_{j\sigma}+\tfrac{1}{2}\sum_{\substack{i,j\\ \sigma,\sigma'}}U_{ij}a_{i\sigma}^{\dagger}a_{i\sigma}a_{j\sigma'}^{\dagger}a_{j\sigma'}\ , \tag{1}$$

where i,j label the Cu and O sites, and the creation (destruction) operators $a_{i\sigma}^{\dagger}$ ($a_{i\sigma}$) explicitly refer to holes with spin σ in the $3d_{x^2-y^2}$ and $2p_x$ ($2p_y$) orbitals (note that we will only consider the p_σ orbitals). The diagonal parameters ($i=j$) are the site energies ε_d and ε_p, and the intrasite Hubbard repulsion energies U_d and U_p. The off-diagonal terms (near neighbor only, for now) are $\varepsilon_{ij}=\pm t$ (the p-d hybridization), and the Coulombic repulsion between holes on neighboring sites $U_{ij}=V$. The vacuum state for this Hamiltonian is the electronic configuration $3d^{10}2p^6$. From now on we shall take $\varepsilon\equiv\varepsilon_p-\varepsilon_d$ to be positive, and thus for a density of one hole per cell the lowest energy state has a hole residing on each Cu site.

In this paper we shall always restrict our attention to the Hilbert space with singly occupied Cu $3d_{x^2-y^2}$ orbitals, as well as one additional hole. As pointed out by Emery,[5] if $U_d>\varepsilon+2V$, the extra hole must reside on an O site. For this restricted Hilbert space we have derived an effective Hamiltonian including all terms that are of order t^2, as well as the Cu-Cu superexchange interaction, which is of order t^4. We find that the effective Hamiltonian[12–16] is given by

$$\begin{aligned}\hat{H}_{\rm eff}=&4J_1{\sum_{\langle ii'\rangle}}'(\mathbf{S}_i\cdot\mathbf{S}_{i'}-\tfrac{1}{4})+4J_2\sum_{\langle il\rangle}(\mathbf{S}_i\cdot\mathbf{S}_l-\tfrac{1}{4}n_l)\\&+(t_a+t_b)\sum_{\substack{\langle l'il\rangle\\ \sigma'\sigma}}[\mathbf{S}_i\cdot(b_{l'\sigma'}^{\dagger}\hat{\tau}_{\sigma'\sigma}b_{l\sigma})+\text{H.c.}]\\&+\frac{t_b-t_a}{2}\sum_{\substack{\langle l'il\rangle\\ \sigma}}(b_{l'\sigma}^{\dagger}b_{l\sigma}+\text{H.c.})\ .\end{aligned} \tag{2}$$

In Eq. (2) we have denoted the Cu and O sites by i and l, respectively, and $\langle ii'\rangle$ and $\langle il\rangle$ represent neighboring Cu and neighboring Cu and O sites, respectively. The local spin operator is given by $\mathbf{S}_i=\frac{1}{2}b_{i\sigma}^{\dagger}\hat{\tau}_{\sigma\sigma'}b_{i\sigma'}$, for either Cu or O, where the $\hat{\tau}$ are Pauli matrices, and the $b_{i\sigma}$ are projected fermionic operators $b_{i\sigma}=a_{i\sigma}(1-n_{i-\sigma})$ that do not allow double occupancy of any orbital. The number operator for site i, spin σ, is denoted by $n_{i\sigma}$, and $n_l=n_{l\sigma}+n_{l-\sigma}$.

The first term in Eq. (2) represents the antiferromagnetic Cu-Cu Heisenberg superexchange, where the primed sum indicates that the Cu—Cu bond possessing the additional O $2p$ hole is to be omitted. (We estimate that the Cu-Cu superexchange of this omitted interaction has an energy that is an order of magnitude less than J_1.) In the large-U limit one may expect

$$J_1 \sim \frac{t^4}{(\varepsilon+V)^2}\left[\frac{1}{U_d}+\frac{2}{U_p+2\varepsilon}\right] . \tag{3}$$

The second summation in Eq. (2) is the superexchange of the O hole with its neighboring Cu spins, for which

$$J_2 \sim \frac{t^2}{2}\left[\frac{1}{U_d-\varepsilon-2V}+\frac{1}{U_p+\varepsilon}\right] . \tag{4}$$

The hole on an O site may hop to any of its six neighboring O sites through the intervening Cu. These processes (lowest order, only) are shown in Fig. 1, and correspond to the last two terms of Eq. (2). The expression $\langle l'il \rangle$ denotes an O-Cu-O near-neighbor triplet (see Fig. 1) of sites. One may estimate t_a and t_b using Rayleigh-Ritz perturbation techniques and find

$$t_a \sim \frac{t^2}{U_d-\varepsilon-2V} , \tag{5}$$

$$t_b \sim \frac{t^2}{\varepsilon} . \tag{6a}$$

However, as pointed out by Emery and Reiter,[15] a better estimate for t_b is obtained via Wigner-Brillouin perturbation theory (which is necessary if t is of the same order of magnitude as ε). They find

$$t_b \sim \frac{1}{2}\left|\frac{\varepsilon}{2}-\left[\left[\frac{\varepsilon}{2}\right]^2+2t^2\right]^{1/2}\right| . \tag{6b}$$

Using the fitting of the extended Hubbard model parameters suggested by Schluter[34] (viz., $\varepsilon=1.5$ eV, $U_d=9$ eV, $U_p=6$ eV, $t=1.4$ eV, and $V=1.6$ eV), one finds the following estimates for these terms:

$$\begin{aligned} J_1 &\sim 0.13 , \\ J_2 &\sim 0.36 , \\ t_a &\sim 0.46 , \\ t_b &\sim 0.68 , \end{aligned} \tag{7}$$

all in eV. This set of values is close to that obtained using other determinations of the extended Hubbard model parameters,[15] and thus we consider Eq. (2) with the above set of values to be typical of a doped CuO_2 plane. However, in order to ensure that our results do not depend sensitively on this choice, we have used other values of J_1, J_2, t_a, and t_b (and also included a direct O-O hybridization, viz., t_{pp}: See Sec. V) for completeness.

Last, implicit in Eq. (2) is the transformation given by Emery and Reiter[15] that produces a purely s-wave character of both the Cu and O orbitals.

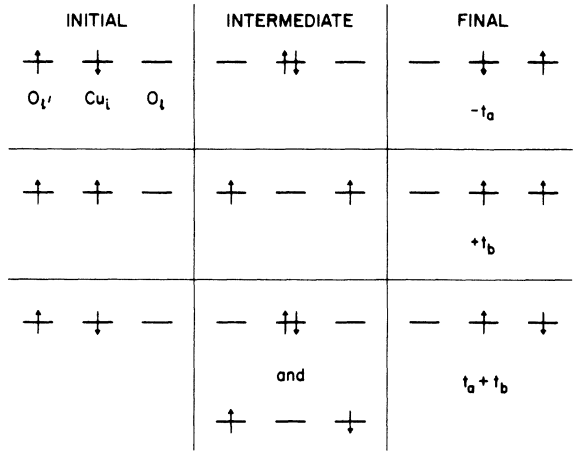

FIG. 1. Three hopping processes of order t^2 in the two-band model. Site l' is the initially occupied O orbital, site i the intermediate Cu orbital, and site l the final O orbitals, in which the O hole resides.

III. Quantum Cluster Studies

The exact quantum ground state of small clusters (16 or 18 sites) proved to be a valuable complement to more analytic and approximate treatments of the properties of one hole in the t-J model. The same is true for the model in Eq. (2). When the hopping is not much larger than the exchange, 16 sites are quite sufficient to describe the core,[35] i.e., the region in which the hole strongly scrambles the local spin arrangement. The numerical calculation will give the ground-state energy at several key points in the Brillouin zone, the symmetry of the "far-field" part of the wave function, and the relative configurations of the Cu and O spins. The latter question sheds light on the structure of the "quasiparticle."

In this section we find the ground state of Eq. (2) by the iterative product method for a 4×4 Cu-O cluster with one hole and a total S^z (to be denoted by S_T^z) of $\frac{1}{2}$. Periodic boundary conditions are used. There is no broken spin-space symmetry in the ground state, in analogy with the Lieb-Schultz-Mattis[36] result for the Heisenberg model, and the lowest total spin state is generally preferred (unless $t_{a,b}/J_1$ is too large). Translational invariance then reduces the number of inequivalent O sites to two, so there are $2\binom{17}{9}=48\,620$ basis states in the $S_T^z=\frac{1}{2}$ sector. The numerical work involved, on average, is a factor of 8 times greater than that of the corresponding t-J cluster.

A representation of our cluster is shown in Fig. 2. The Cu states form a square lattice $i=m\hat{\mathbf{x}}+n\hat{\mathbf{y}}$, and there are two O basis sites at $\frac{1}{2}\hat{\mathbf{x}}$ and $\frac{1}{2}\hat{\mathbf{y}}$ in each unit cell. By convention, we assume that the hole is always between site 1 and 2, or 1 and 8.

The mean-square AF order parameter is

$$\langle \hat{\Omega}^2 \rangle = \frac{4}{N^2}\left\langle \left[\sum_i \epsilon_i \mathbf{S}_i\right]^2 \right\rangle , \tag{8}$$

where $\epsilon_i=1$ for an A sublattice site, and $\epsilon_i=-1$ for a B

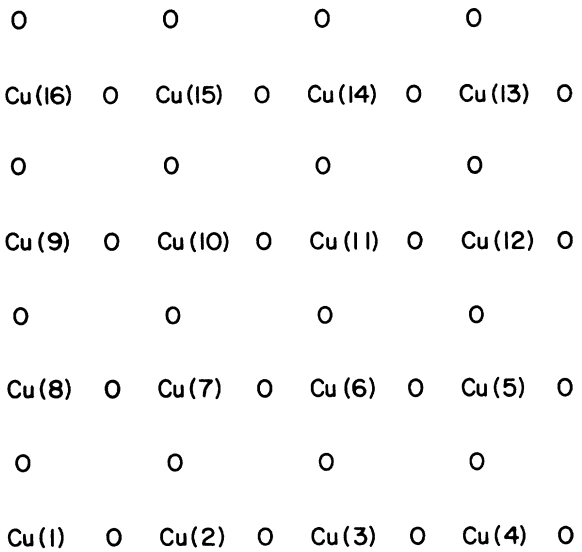

FIG. 2. 4×4 CuO_2 cluster, and the labeling of the Cu sites, used in the quantum cluster studies.

sublattice site (recall that a square lattice is bipartite). For the classical Néel configuration this order parameter is equal to 1. The value on a 16-site cluster is slightly larger, 1.106, in spite of the quantum fluctuations, since N terms in the square are just $\mathbf{S}_i^2$, which is three times the corresponding value in the Ising limit.

There are a large number of parameters in this problem, and it is helpful to first consider the limit $t_a=t_b=0$, viz., a quenched hole in Sec. III A, before turning on the hopping in Sec. III B. Since the relation between the total spin, the AF order parameter, the O spin, and the Cu spins near the hole is quite complex, we organize our numerical output by stating in each subsection a semiclassical model that reproduces qualitatively our quantum measurements. In Sec. IV this model is developed more deductively and quantitatively.

A. Quenched hole

When $t_a=t_b=0$, the O $2p$ hole will reside on a single site which we take to be (1-2). Its spin is not conserved, however, and there is just one relevant parameter in Eq. (2), J_2/J_1. This limit may be of some experimental interest since a small amount of doping leaves the parent superconductivity compound insulating.[37] If the disorder tightly localizes the extra hole to a single O site, then the considerations of this section should apply.

Aharony *et al.*[18] have considered the classical x-y version of this problem. Far from the hole, imagine that the spins on the two sublattices are along $\hat{\mathbf{y}}$, $\mathbf{S}^0_{A,B}=\pm\frac{1}{2}\hat{\mathbf{y}}$. By symmetry the optimal configuration for the O spin is the x direction. Then observe that the J_2 Cu-O exchange forces the two adjacent A,B Cu spins to develop components antiparallel to the O spin. This distortion then perturbs the remaining spins so that the ground state is described by $\mathbf{S}_{A(B)}\sim\mathbf{S}^0_{A(B)}\pm[\mathbf{p}\cdot\hat{\mathbf{r}}f(r)]\hat{\mathbf{x}}$, where $\mathbf{p}=p\hat{\mathbf{u}}$, $\mathbf{r}$ is the location of $\mathbf{S}_{A(B)}$ relative to the hole, f decreases with r and behaves like r^{-1} for large r, and $\mu=\mathbf{x},\mathbf{y}$ corresponds to the two inequivalent locations of the O hole in a unit cell (which result in two distinct distortion patterns). The far-field distortion then has a dipolar form with the dipole moment $\mathbf{p}=p\hat{\boldsymbol{\mu}}$, which is aligned along the occupied bond and has a magnitude p depending on J_2/J_1. The spin distortion occurs in direction $\hat{\mathbf{x}}$ in spin space, which one notes is parallel to $\mathbf{S}_O$ and perpendicular to the far-field staggered magnetization $\hat{\boldsymbol{\Omega}}=\hat{\mathbf{y}}$. Hence in the coordinate independent form the distortion can be parametrized by an *antiferromagnetic* dipole moment[22] defined as $\mathbf{P}_a\equiv p_a\mathbf{S}_O\times\hat{\boldsymbol{\Omega}}$, where $a=x,y$ is a real-space index. Clearly, $\mathbf{P}_a$ is a bivector in the lattice and spin space. The far-field spin distortion can then be expressed in the form

$$\delta(\mathbf{S}_A-\mathbf{S}_B)\sim\sum_a\frac{r_a}{r^2}\mathbf{P}_a\times\hat{\boldsymbol{\Omega}}\ . \tag{9}$$

We have found that when suitably interpreted, this classical picture is essentially correct in the quenched limit. Significant elaboration is necessary since the quantum ground state is rotationally invariance around $\hat{\mathbf{z}}$, and only the magnitude of the order parameter is defined, not its direction. More complicated matrix elements are therefore necessary to uncover the correlations we seek. We first enumerate and discuss the relevant correlation functions and symmetries, and then turn to their evaluation.

Spin overlaps $\langle\mathbf{S}_i\cdot\mathbf{S}_{i'}\rangle$ and z components such as $\langle S^z_O\rangle$ are all easy to compare with the classical limit. The correlation between the hole and the two adjacent Cu is clearly trivial for $J_2=0$, while for $J_2\gg J_1$, as observed by Emery and Reiter,[15] it follows from diagonalizing

$$\mathbf{H}_3=4J_2\mathbf{S}_O\cdot(\mathbf{S}_{\mathrm{Cu}(1)}+\mathbf{S}_{\mathrm{Cu}(2)})\ . \tag{10a}$$

The so-called 3-spin polaron is the doubly degenerate, total spin $\frac{1}{2}$, ground state of this Hamiltonian. The $S^z_T=+\frac{1}{2}$ state has the form

$$|\psi_0\rangle=\frac{1}{\sqrt{6}}(2|\uparrow\downarrow\uparrow\rangle-|\uparrow\uparrow\downarrow\rangle-|\downarrow\uparrow\uparrow\rangle)\ , \tag{10b}$$

where each of the kets refers to the spins occupying the Cu(1)–O–Cu(2) bond. It will evidently be of interest to project the complete density matrix onto the 2^3 basis states relevant to $\mathbf{H}_3$, and then find the weight in the 3-spin polaron as a function of J_2/J_1. (For the mobile hole, we will also examine the weight in the spin singlet state proposed by Zhang and Rice.)

A convenient measure of the relative orientation of Cu spin is $\langle(\mathbf{S}_i\times\mathbf{S}_{i'})_z\rangle$, where only the z component survives by rotational symmetry. In the classical configuration given in Eq. (9) this cross product is along $\hat{\mathbf{z}}$, and has dipolar symmetry.[22,38] Its physical interpretation is a bond spin current, as follows from the equations of motion:

$$\begin{aligned}
\frac{\partial \mathbf{S}_O}{\partial t} &= -4J_2(\mathbf{S}_O\times\mathbf{S}_1+\mathbf{S}_O\times\mathbf{S}_2)\ , \\
\frac{\partial \mathbf{S}_1}{\partial t} &= -4J_2\mathbf{S}_1\times\mathbf{S}_O-4J_1\sum_{i\in\langle i,1\rangle}{}'\ \mathbf{S}_1\times\mathbf{S}_i\ , \\
\frac{\partial \mathbf{S}_2}{\partial t} &= -4J_2\mathbf{S}_2\times\mathbf{S}_O-4J_1\sum_{i\in\langle i,2\rangle}{}'\ \mathbf{S}_2\times\mathbf{S}_i\ , \\
\frac{\partial \mathbf{S}_i}{\partial t} &= -4J_1\sum_{\substack{i'\in\langle ii'\rangle \\ i\neq 1,2}}\mathbf{S}_i\times\mathbf{S}_{i'}\ .
\end{aligned} \tag{11}$$

The prime on the second and third sums indicates the absence of the term corresponding to the occupied Cu(1)—O—Cu(2) bond. The sum of the right-hand sides of the four lines in Eq. (11) is, of course, zero, since the total spin is conserved, and the expectation value of any time derivative in the ground state is zero. Thus the presence of the O spin acts as a "source" for $\mathbf{S}_i\times\mathbf{S}_{i'}$ which would otherwise be zero.

Although $\langle(\mathbf{S}_i\times\mathbf{S}_{i'})_z\rangle$ will be useful in characterizing the distortion due to a mobile hole, additional symmetries make this expectation value zero in the quenched case. Specifically, because (i) there is no broken AF symmetry, and (ii) the total spin is along $\hat{\mathbf{z}}$, the product of a spin rotation by π around $\hat{\mathbf{y}}$ followed by time reversal is a symmetry of the ground state. It has the effect of reversing just the y components of the spins, thus $\langle(\mathbf{S}_i\times\mathbf{S}_{i'})_z\rangle=0$. The same argument implies that all triple products, such as $\langle\mathbf{S}_O\cdot(\mathbf{S}_i\times\mathbf{S}_{i'})\rangle=0$. To circumvent this problem we must refer $(\mathbf{S}_i\times\mathbf{S}_{i'})$ to some other vector in spin space. Two obvious correlations are $\langle(\boldsymbol{\Omega}\times(\mathbf{S}_i\times\mathbf{S}_{i'}))_z\rangle$ and $\langle(\mathbf{S}_O\times\boldsymbol{\Omega})\cdot(\mathbf{S}_i\times\mathbf{S}_{i'})\rangle$, which are not required by symmetry to vanish.

In Table I we display several matrix elements that measure, in various ways, the AF correlations as a function of increasing J_2/J_1. The two Cu spins adjacent to the hole (1,2), even for $J_2=0$ decorrelate slightly with respect to the Heisenberg AF model, since the corresponding Cu-Cu exchange term is absent. For large J_2, $\langle\mathbf{S}_1\cdot\mathbf{S}_2\rangle$ approaches its ferromagnetic limit of $+\frac{1}{4}$. For more reasonable values of J_2 the destruction of AF correlations is quite localized, as is seen from the values[39] of $\langle\mathbf{S}_2\cdot\mathbf{S}_3\rangle$ and $\langle\Omega^2\rangle$.

The value of $\langle S_O^z\rangle$ is suggestive as to where the total spin resides, and is indicative of how the system would respond to a magnetic field. When $J_2=0$ the "excess" spin $\frac{1}{2}$ is all on O, $\langle S_O^z\rangle=\frac{1}{2}$, and the 16 Cu spins are in a total spin singlet. For large J_2/J_1, $\langle S_O^z\rangle$ is nearly $-\frac{1}{6}$, which is the value expected for the 3-spin polaron with $S_T^z=+\frac{1}{2}$ [cf. Eq. (10b)]. In other words, the O spin is forced down by the adjacent Cu spins, which are becoming parallel, and prefer to be up. For intermediate J_2/J_1 we have found a jump in $\langle S_O^z\rangle$ from positive to negative values due to a level crossing; this may only be a finite-size effect. The evolution of the total probability in the two spin states of the 3-spin polaron is much smoother, as the last column of Table I shows. For a random wave function this probability would be 25%, so that the value of 92% found for $J_2/J_1=3$ is quite appreciable. Hence, for $J_2/J_1>3$ one may think of the three Cu(1)-O-Cu(2) spins as forming a single effective spin-$\frac{1}{2}$ object. This polaron has six nearest-neighbor Cu spins, three from each sublattice, and with each of which experiences an exchange interaction of $J_{\text{eff}}=\frac{2}{3}J_1$. From simple perturbation theory we therefore expect the weight in the polaron state to converge to 1 as $J_1/J_2\to 0$.

The value of $\langle S_O^z\rangle$ is more subtle and can deviate from $-\frac{1}{6}$ because of the finite probability that the 14 remaining Cu spins have $\langle S_T^z\rangle=+1$. The latter is related to the singlet-triplet gap for a Heisenberg QAF lattice versus the effective exchange J_{eff}. There are no obvious factors of J_2/J_1 in this comparison which makes analytic estimates difficult.

To measure the dipole moment we display in Table II

$$\langle(\mathbf{S}_O\times\boldsymbol{\Omega})\cdot(\mathbf{S}_i\times\mathbf{S}_{i'})\rangle/\langle(\mathbf{S}_O\times\boldsymbol{\Omega})^2\rangle^{1/2}$$

for the bonds (1,2) and (2,3). For the spins which surround the hole, this correlation is maximum at $J_2/J_1\sim 2$, and then decreases; in semiclassical terms, the two Cu spins are becoming parallel and the cross product vanishes. For the bond adjacent to the hole this quantity saturates with increasing J_2/J_1, in analogy with the classical behavior.[18] When other values of (ii') are examined the dipolar symmetry becomes obvious, with the spatial direction of AF dipole moment parallel to the bond occupied by the hole. Finally, $\langle(\boldsymbol{\Omega}\times(\mathbf{S}_i\times\mathbf{S}_{i'}))_z\rangle$ adds little that is new since it is roughly proportional to

$$\langle(\mathbf{S}_O\times\boldsymbol{\Omega})\cdot(\mathbf{S}_i\times\mathbf{S}_{i'})\rangle/\langle S_O^z\rangle\ .$$

The signs of these correlation functions, as well as a ra-

TABLE I. Various measures of the spin arrangement around a quenched hole. The polaron weights include both polaron states. The O hole is localized on the (1,2) bond (see Fig. 2 for site labeling).

J_2/J_1	$\langle\mathbf{S}_1\cdot\mathbf{S}_2\rangle$	$\langle\mathbf{S}_2\cdot\mathbf{S}_3\rangle$	$\langle\hat{\boldsymbol{\Omega}}^2\rangle$	$\langle S_O^z\rangle$	3-spin polaron occupation (%)
4×4 QAF	−0.3509	−0.3509	1.106		
0	−0.2051	−0.3821	1.095	+0.5	18.2
1	−0.1246	−0.3590	1.065	+0.438	44.7
2	+0.0420	−0.2933	0.990	+0.290	73.1
3	+0.1793	−0.1371	0.945	−0.162	92.1
6	+0.2278	−0.0896	0.909	−0.160	97.6
25	+0.2485	−0.0483	0.877	−0.158	99.8

TABLE II. Two measures of the spin twist around a quenched hole, as defined by the correlation function $\langle(\mathbf{S}_O\times\mathbf{\Omega})\cdot(\mathbf{S}_i\times\mathbf{S}_{i'})\rangle/\langle(\mathbf{S}_O\times\mathbf{\Omega})^2\rangle^{1/2}$, for $(i,i')=(1,2),(2,3)$.

J_2/J_1	$\frac{\langle(\mathbf{S}_O\times\mathbf{\Omega})\cdot(\mathbf{S}_1\times\mathbf{S}_2)\rangle}{\langle(\mathbf{S}_O\times\mathbf{\Omega})^2\rangle^{1/2}}$	$\frac{\langle(\mathbf{S}_O\times\mathbf{\Omega})\cdot(\mathbf{S}_2\times\mathbf{S}_3)\rangle}{\langle(\mathbf{S}_O\times\mathbf{\Omega})^2\rangle^{1/2}}$
1	+0.1853	−0.0852
2	+0.2824	−0.1541
3	+0.2609	−0.2417
6	+0.1977	−0.2422
25	+0.1232	−0.2383

tionale for those which vanish, follow from the semiclassical spin arrangement in Fig. 3. All spins, including S_T^z, are coplanar, and the figure must be averaged around $\hat{\mathbf{z}}$ to restore rotational symmetry. From the figure it is then evident that $\langle\mathbf{S}_O\cdot(\mathbf{S}_i\times\mathbf{S}_{i'})\rangle=0$ and $\langle(\mathbf{S}_i\times\mathbf{S}_{i'})_z\rangle=0$, while $\langle(\mathbf{S}_O\times\mathbf{\Omega})\cdot(\mathbf{S}_i\times\mathbf{S}_{i'})\rangle$ captures precisely the twist in $\mathbf{S}_i$ from site to site.

B. Mobile hole

We now consider the full Hamiltonian given in Eq. (2), viz., $t_a\neq0$, $t_b\neq0$. By virtue of the periodicity, the exact many-particle wave function has a Bloch index $\mathbf{k}$, and it acquires the usual phase factor when translated by one lattice site. The hole can occupy any site, but to minimize the number of basis states in the numerics we can exploit the translations to place the hole on either the x bond (1,2) or the y bond (1,8).

Due to the finite size of the cluster, and the periodic boundary conditions that we impose, there are only six independent $|\psi_{\mathbf{k}}\rangle$, modulo spatial symmetries, that may be studied: $\mathbf{k}=0$, $(\pi/2,0)$, $(\pi,0)$, $(\pi,\pi/2)$, (π,π), and $(\pi/2,\pi/2)$. A further finite-size effect (particular to 4×4 clusters: see Appendix A) leads to a degeneracy of the $\mathbf{k}=(\pi,0)$ and $(\pi/2,\pi/2)$ states.

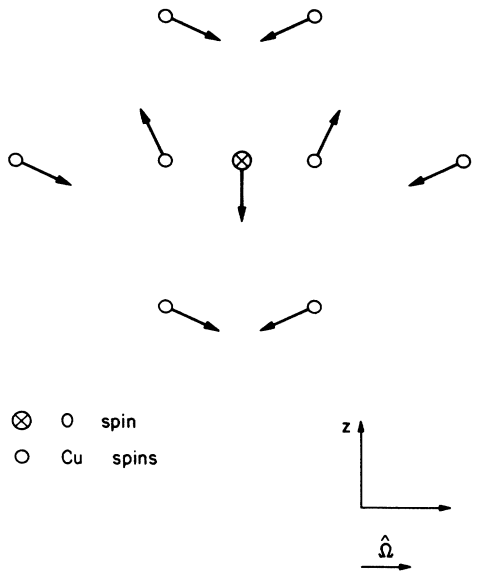

FIG. 3. Semiclassical spin configuration in the neighborhood of the quenched hole. All the spins are coplanar, and the total spin is in the z direction. The entire picture must be rotationally averaged around the z axis in order to compare to our quantum cluster studies.

The correlation functions, in particular, $\langle(\mathbf{S}_i\times\mathbf{S}_{i'})_z\rangle$ for the mobile hole are very different from the previous case. The symmetry argument in the quenched limit employed a global spin rotation plus time reversal to show that $\langle(\mathbf{S}_i\times\mathbf{S}_{i'})_z\rangle$ vanishes. Now time reversal sends $\mathbf{k}\rightarrow-\mathbf{k}$. The states $(\pi,0)$ and $(-\pi,0)$ differ by a reciprocal lattice vector and are therefore identical, hence $\langle(\mathbf{S}_i\times\mathbf{S}_{i'})_z\rangle$ remains zero. However, $(\pi/2,\pi/2)$ and $(-\pi/2,-\pi/2)$ are not identical since there is no broken magnetic symmetry and (π,π) is not a reciprocal lattice vector; therefore, the corresponding bond spin current need not vanish. The same result follows alternatively by realizing that a spin current must have both a spin and a spatial index. For the $(\pi,0)$ state no spatial vector exists, while for other values of $\mathbf{k}$, one does. One is therefore able to observe that the bond spin currents may have a dipolar dependence on space, with a dipole moment determined by $\mathbf{k}$. Identical reasoning was employed for the t-J model.[22]

The total spin of the lowest energy state for all $\mathbf{k}$ is $\frac{1}{2}$. Our 4×4 calculations for Eq. (2) show unambiguously that the bottom of the O hole band lies on the zone boundary. However, an accidental symmetry of the 4×4 cluster (see Appendix A) makes the $(\pi/2,\pi/2)$ and $(\pi,0)$ points of the Brillouin zone degenerate, and the exact location of the energy minimum along the zone boundary remains undetermined. While the semiclassical study (see Sec. IV) shows that the long-ranged distortions of the spin field favor $(\pi/2,\pi/2)$ over $(\pi,0)$, this by itself could not produce a necessarily correct conclusion. The direct O-O hopping considered in Sec. V breaks the special 4×4 symmetry, and definitely places the minimum energy at $(\pi/2,\pi/2)$. This conclusion is consistent with the study of the 10-site cluster by Shiba and Ogata.[29]

To test the sensitivity of these results to the specific parameters in Eq. (7), we have recalculated the ground state for a sequence of values of J_1, J_2, t_a, and t_b, assumed to be independent, i.e., ignoring Eqs. (3)–(6). To be specific, we have individually varied each of these parameters by a factor of 2 up and down (e.g., for J_1 we have studied the values 0.065, 0.13, and 0.26, eV, while keeping the values of J_2, t_a, and t_b fixed). No change in the above-stated characteristics of the ground state was found.

The width of the lowest energy band (which in practice was the energy at $\mathbf{k}=0$ versus zone boundary) is 0.98 eV for the standard parameters in Eq. (7). In Fig. 4 we show this width as a function of J_1, as well as γt_a, γt_b, $\gamma=1$, 2, 3. In the regime $J_1\ll t$ the bandwidth is a linear function of J_1, and is independent of t_a and t_b. Analogous behavior was found in the one-band model.[22–25]

We now look at the local O-hole quasiparticle structure in our system. We have calculated $\langle S_O^z\rangle$ for all states studied. Recall that for a quenched hole this expectation value varied from $+\frac{1}{2}$ to approximately $-\frac{1}{6}$ (for J_2 being varied from 0 to ∞), as shown in Table I. However, for the mobile hole and standard parameters

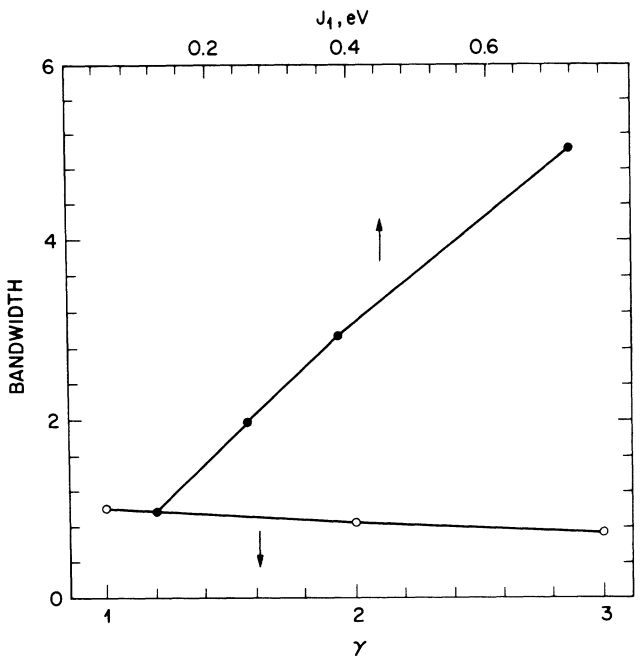

FIG. 4. Variation of the bandwidth as a function of J_1, as well as $\gamma \equiv t_a/0.46$ eV, where the ratio t_a/t_b is fixed.

we find the interesting result[17,31] $\langle S_O^z \rangle = 0 \pm 0.003$ (see Table III). Clearly large hopping is necessary to force $\langle S_O^z \rangle$ to zero (and some amount of Cu-O exchange enhances this process). We also observed this behavior in a study of the one-dimensional version of Eq. (2), for sufficiently long chains. The extra $\hat{z}$ magnetization is taken up by the canting of the Cu spins, as is shown on Fig. 5(b) [cf. the Cu spin expectation values for the quenched hole are shown in Fig. 5(a)].

In Sec. III A the 3-spin polaron was found to be the dominant configuration around the hole for $J_2/J_1 \gtrsim 3$, and one would want to know whether it is compatible with the hopping. Table III shows the relevant projections. The addition of the hopping for $J_2/J_1 = 3$ changes the weight negligibly, from 92% in the quenched case, to 90% for Eq. (7). Moreover, comparing this value with the weights for the $J_2 = 0$ and $J_2/J_1 = 10$ states show that

(a)

-0.0242	-0.0242	0.0374	0.0374
0.0374	0.0374	0.0024	0.0024
-0.0242	-0.0242	0.0374	0.0374
0.2889	0.2889	-0.0242	-0.0242

(b)

0.0351	0.0354	0.0179	0.0233
0.0236	0.0236	0.0219	0.0220
0.0354	0.0350	0.0233	0.0179
0.0489	0.0489	0.0422	0.0422

FIG. 5. Expectation values of Cu spins $\langle S_i^z \rangle$ are shown. In (a), the results for quenched hole at $J_2/J_1 = 3$ are shown, while in (b) we present the results for mobile hole at $\mathbf{k} = (\pi/2, \pi/2)$, for the parameter values of Eq. (7). In (b), the expectation values are taken with the complete Bloch state, where projection operators are utilized which project the hole onto the O site on bond (1,2) [see Eq. (2) for Cu-site labeling].

the hopping itself favors the polaron. However, it is difficult to increase the polaron occupancy to 100% just by increasing the hopping. (Recall that in Table I, the weights in the nonpolaron states decreased more rapidly than J_2/J_1 as the latter tended to zero.) The weights in the individual $S^z = \pm\frac{1}{2}$ polaron spin states are 53.6 and 36.4 % for the standard parameters. They become more nearly equal when the hopping increases, but $\langle S_O^z \rangle$ remains a factor 10 closer to zero than these probabilities would suggest. Another open question is why $\langle S_O^z \rangle$ is of order a few percent when $\mathbf{k} \neq 0$ and not on the zone boundary. Hence the 3-spin polaron is not capturing all the physics we find in the ground state.

The polaron was the obvious "quasiparticle" in the limit of $J_2/J_1 \to \infty$ with no hopping. Another simple limit is to restrict the hopping to the four O sites that surround a common Cu site, and diagonalize Eq. (2) within this cluster.[11] The ground state is evidently symmetric under rotations about the central copper, and is a spin singlet. One can again take the full wave function and project onto the 2^4 states describing this cluster. In Table III we show the weight in the ground state which is dominant, as well as the weight in the next most probable state, a spin triplet with p-wave symmetry. This nearest-neighbor Zhang-Rice state (not their Wannier state) is

TABLE III. Several measures of the spin arrangement around a mobile hole for the standard parameters [see Eq. (7)], and $\mathbf{k} = (\pi/2, \pi/2)$, except as noted. The polaron weights include both spin states. The remaining two columns show the weights in the spin singlet, spatially symmetric state of a CuO_4 cluster (Ref. 11), as well as the spin triplet spatial p-wave states. [The p states include just the one state proportional to $(1,1,-1,-1)$ for $\mathbf{k} = (\pi/2, \pi/2)$, but all three for $\mathbf{k} = 0$.]

Parameter values	$\langle S_O^z \rangle$	3-spin polaron occupation (%)	Zhang-Rice singlet occupation (%)	Triplet, p-wave occupation (%)
$J_2 = 0$	0.015	85.9	63.7	22.7
$J_2 = 0.13$	0.010	87.6	64.3	21.5
Eq. (7) values	0.003	90.1	65.1	19.9
$J_2 = 1.3$	−0.010	95.2	66.1	16.2
$t_a = 1.38$ $t_b = 2.04$	$< 10^{-3}$	91.8	67.0	15.9
$\mathbf{k} = (0,0)$	$< 10^{-3}$	90.6	65.4	19.9

not as good an approximation to the exact ground state projected onto its subspace as is the polaron for the corresponding projection subspace, but the two descriptions are somewhat complementary. Further, one expects a larger projection onto such a singlet with next-nearest neighbor sites included. We shall return to this point in the conclusion.

In order to further illustrate the distribution of spins in these states, we can examine the partitioning of the total spin between oxygen and all the coppers taken together. We have seen that the states have total $S_T=\frac{1}{2}$ and $\langle S_O^z\rangle=0$. We then calculated the total copper spin $\langle \mathbf{S}_{Cu}^2\rangle=\langle(\sum_{i=1}^{16}\mathbf{S}_i)^2\rangle$. For all $\mathbf{k}$, and for the parameters given in Eq. (7), we find $\langle \mathbf{S}_{Cu}^2\rangle=1.5\pm0.01$. These three numbers, $S_T=\frac{1}{2}$, $\langle S_O^z\rangle=0$, and $\langle \mathbf{S}_{Cu}^2\rangle=1.5$ are not independent, and may be understood as follows. The total Cu spin must be 0 or 1 to give $S_T=\frac{1}{2}$. For those components of the ground state for which $S_O^z=-0.5$, the total S^z of the Cu spins, S_{Cu}^z, must be 1, along with the total Cu spin S_{Cu}. For the components of the ground state for which $S_O^z=0.5$, $S_{Cu}^z=0$; so it can be a linear combination of $S_{Cu}=0$, and $S_{Cu}=1$ states. In order that the $S_{Cu}=1$ states (the $S_{Cu}^z=0,1$ states) combine with the O hole's spin to form a $S=\frac{1}{2}$ state, the required linear combination of $|S_{Cu},S_{Cu}^z\rangle_{Cu}|S_O,S_O^z\rangle_O$ states is

$$(|1,0\rangle_{Cu}|\tfrac{1}{2},\tfrac{1}{2}\rangle_O-\sqrt{2}|1,1\rangle_{Cu}|\tfrac{1}{2},-\tfrac{1}{2}\rangle_O)/\sqrt{3}\ . \quad (12a)$$

Further, since $\langle S_O^z\rangle=0$ is observed, consistency requires that a 3:1 ratio of the $S_{Cu}=1$, and 0 states be present in the ground state. To be specific, we predict that the ground state $|\psi_G\rangle$ may be written as

$$|\psi_G\rangle=\tfrac{1}{2}|0,0\rangle_{Cu}|\tfrac{1}{2},\tfrac{1}{2}\rangle_O + e^{i\phi}\frac{\sqrt{3}}{2}\frac{|1,0\rangle_{Cu}|\frac{1}{2},\frac{1}{2}\rangle_O-\sqrt{2}|1,1\rangle_{Cu}|\frac{1}{2},-\frac{1}{2}\rangle_O}{\sqrt{3}}\ , \quad (12b)$$

where ϕ is an undetermined (real) phase. Note that for this state

$$\begin{aligned}&\langle\psi_G|S_O^z|\psi_G\rangle=0\ ,\\ &\langle\psi_G|\mathbf{S}_T^2|\psi_G\rangle=0.75\ ,\\ &\langle\psi_G|\mathbf{S}_{Cu}^2|\psi_G\rangle=1.5\ ,\end{aligned} \quad (12c)$$

precisely what we find numerically. For parameter values other than Eq. (7), e.g., $J_2=0$, (cf. Table III), $\langle \mathbf{S}_{Cu}^2\rangle=1.460$, showing that when $\langle S_O^z\rangle$ is larger than zero $\langle \mathbf{S}_{Cu}^2\rangle$ decreases.

We have found two reasonable measures for the distortion of the background Cu spins: $\langle(\mathbf{S}_O\times\mathbf{\Omega})\cdot(\mathbf{S}_i\times\mathbf{S}_{i'})\rangle$ that we studied in Sec. III A, and $\langle(\mathbf{S}_i\times\mathbf{S}_{i'})_z\rangle$ which is now nonzero for $\mathbf{k}\neq0,(\pi,0)$. They will be examined systematically as a function of J_2/J_1 and $(t_a+t_b)/J_1$, but mainly for $\mathbf{k}=(\pi/2,\pi/2)$. In general, we find the same tendencies as for the 3-spin polaron occupations, namely, that either the hopping or the Cu-O exchange will saturate the dipole moment.

In Fig. 6(a) we show the bond spin currents $\langle(\mathbf{S}_i\times\mathbf{S}_{i'})_z\rangle$ for the standard parameters given in Eq. (7) and the wave function with the hole occupying any four of the O sites adjacent to Cu-1 site (cf. Fig. 2). The currents are even when reflected across the lines running diagonally from site 1, either parallel or perpendicular to $\mathbf{k}$. The magnitudes and signs of the bond *currents* have a clear quadrupole component. This demonstrates the dipole symmetry of the Cu *spin* distortions. It is necessary

+0.003 −0.047 +0.020 +0.021

Cu −0.047 Cu +0.030 Cu +0.042 Cu +0.021

+0.091 +0.030 +0.027 +0.042

Cu −0.020 Cu +0.027 Cu +0.027 Cu −0.020

+0.091 +0.042 +0.027 +0.030

Cu +0.021 Cu +0.042 Cu +0.030 Cu −0.047

+0.003 +0.021 −0.020 −0.047

Cu +0.003 Cu +0.091 Cu +0.091 Cu +0.003

(a)

+0.058 +0.096 +0.022 −0.036

Cu +0.096 Cu −0.022 Cu −0.026 Cu −0.036

−0.095 −0.022 −0.022 −0.026

Cu +0.022 Cu −0.022 Cu −0.022 Cu +0.022

−0.095 −0.026 −0.022 −0.022

Cu −0.036 Cu −0.026 Cu −0.022 Cu +0.096

+0.058 −0.036 +0.022 +0.096

Cu +0.058 Cu −0.095 Cu −0.095 Cu +0.058

(b)

FIG. 6. Correlation functions based on vector products $(\mathbf{S}_i\times\mathbf{S}_j)$ for i and j being near-neighbor Cu sites, at $\mathbf{k}=(\pi/2,\pi/2)$, for the parameter values of Eq. (7). In (a) $\langle(\mathbf{S}_i\times\mathbf{S}_j)_z\rangle$ are shown, while in (b) we present $\langle(\mathbf{S}_O\times\mathbf{\Omega})\cdot(\mathbf{S}_i\times\mathbf{S}_j)\rangle/\langle(\mathbf{S}_O\times\mathbf{\Omega})^2\rangle^{1/2}$. The expectation values are taken with the complete Bloch state, where projection operators are utilized which project the hole onto the four O sites surrounding the Cu-site 1.

TABLE IV. Several measures of the spin twist and dipole moment for a mobile hole. Parameters are standard, except as noted. The second and third columns denote the same correlation function as in Table II, while the next two are the bond spin currents for the same two bonds. The hole is projected onto the bond (1,2) by the operator $\hat{\mathbf{n}}_x$ so as to compare with Table II. The dipole moment P_x is defined in Eq. (16) below.

Parameter values	$\frac{\langle \hat{\mathbf{n}}_x(\mathbf{S}_O\times\boldsymbol{\Omega})\cdot(\mathbf{S}_1\times\mathbf{S}_2)\rangle}{\langle \hat{\mathbf{n}}_x\rangle\langle(\mathbf{S}_O\times\boldsymbol{\Omega})^2\rangle^{1/2}}$	$\frac{\langle \hat{\mathbf{n}}_x(\mathbf{S}_O\times\boldsymbol{\Omega})\cdot(\mathbf{S}_2\times\mathbf{S}_3)\rangle}{\langle(\hat{\mathbf{n}}_x\rangle\langle(\mathbf{S}_O\times\boldsymbol{\Omega})^2\rangle^{1/2}}$	$\frac{\langle \hat{\mathbf{n}}_x(\mathbf{S}_1\times\mathbf{S}_2)_z\rangle}{\langle \hat{\mathbf{n}}_x\rangle}$	$\frac{\langle \hat{\mathbf{n}}_x(\mathbf{S}_2\times\mathbf{S}_3)_z\rangle}{\langle \hat{\mathbf{n}}_x\rangle}$	P_x
$J_2=0$	+0.304	−0.155	−0.093	+0.096	+1.02
$J_2=0.13$	+0.296	−0.157	−0.086	+0.097	+1.34
Eq. (7) values	+0.281	−0.160	−0.076	+0.098	+1.77
$J_2=1.3$	+0.236	−0.166	−0.050	+0.100	+2.73
$t_a=0.016$ $t_b=0.010$	+0.271	−0.210	−0.103	+0.115	+1.44
$t_a=0.05$ $t_b=0.03$	+0.276	−0.199	−0.106	+0.115	+1.54
$t_a=0.10$ $t_b=0.16$	+0.283	−0.185	−0.103	+0.112	+1.69
$t_a=0.20$ $t_b=0.29$	+0.283	−0.173	−0.095	+0.108	+1.74
$t_a=0.26$ $t_b=0.52$	+0.283	−0.167	−0.087	+0.104	+1.85

to run the lines of reflection through site 1 in order to respect the occupations of the O sites. In Fig. 6(b) we show the bond spin currents projected along $(\mathbf{S}_O\times\boldsymbol{\Omega})$.

In Table IV the bond spin currents for $(i,i')=(1,2)$ and (2,3) are shown for a variety of parameters. If either the hopping is reduced at fixed J_2, or vice versa, the spin twist is largely unaffected.

The limit $t_{a,b}\to 0$ is, of course, singular, both because certain correlation functions, e.g., $\langle(\mathbf{S}_i\times\mathbf{S}_{i'})_z\rangle$ vanish by symmetry, but also since so long as hopping is permitted, both O sites in the unit cell will be occupied and the dipole moment in the far field is governed by the wave vector $\mathbf{k}$ rather than the bond direction $\hat{\boldsymbol{\mu}}$. However, we can also recompute our correlation functions conditioned on the location of the O hole, in which case, for $(t_a+t_b)<J_1$ and near to the hole, they resemble what we found in the quenched hole case. Far from the hole, its location should not matter to the bond spin currents; however, the small-t limit is manifest by a long healing length $l\sim[J_1/(t_a+t_b)]^{1/2}$ (cf. Sec. IV) which characterizes the crossover from near- to far-field behavior.

The dual origins of the Cu spin distortion, hopping and Cu-O exchange, can be displayed by generalizing Eq. (11) to include the effects of hopping and employing the same reasoning as before. To be specific, we define a spin density only on the Cu lattice by assigning half of the O spin to each of its adjacent Cu sites,

$$\mathbf{M}_i=\mathbf{S}_i+\tfrac{1}{2}\sum_{l\in\langle il\rangle} b_{l\alpha}^{\dagger}\left[\frac{\hat{\tau}}{2}\right]_{\alpha\beta} b_{l\beta}\ . \tag{13}$$

Commuting $\mathbf{M}_i$ with the Hamiltonian (2), we obtain

$$\frac{\partial \mathbf{M}_i}{\partial t}=-\sum_{i'\in\langle ii'\rangle}\mathbf{J}_{ii'}\ , \tag{14}$$

where $\mathbf{J}_{ii'}$ is a magnetization current "flowing" on the bond (ii'), and which is given by

$$\begin{aligned}\mathbf{J}_{ii'}=&4J_1\mathbf{S}_1\times\mathbf{S}_{i'}+J_2(\mathbf{S}_i-\mathbf{S}_{i'})\times(b_l^{\dagger}\hat{\tau}b_l)+\frac{(t_a+t_b)}{4}\sum_{\langle l'ili'\rangle}\mathbf{S}_i\times(b_{l'}^{\dagger}\hat{\tau}b_l+b_l^{\dagger}\hat{\tau}b_{l'})\\&-\frac{(t_a+t_b)}{4}\sum_{\langle ili'l'\rangle}\mathbf{S}_{i'}\times(b_{l'}^{\dagger}\hat{\tau}b_l+b_l^{\dagger}\hat{\tau}b_{l'})-i\frac{t_a+t_b}{4}\left[\sum_{\langle ili'l'\rangle}\mathbf{S}_{i'}(b_{l'}^{\dagger}b_l-b_l^{\dagger}b_{l'})-\sum_{\langle l'ili'\rangle}\mathbf{S}_i(b_{l'}^{\dagger}b_l-b_l^{\dagger}b_{l'})\right]\\&-i\frac{t_b-t_a}{8}\left[\sum_{\langle ili'l'\rangle}(b_{l'}^{\dagger}\hat{\tau}b_l-b_l^{\dagger}\hat{\tau}b_{l'})-\sum_{\langle l'ili'\rangle}(b_{l'}^{\dagger}\hat{\tau}b_l-b_l^{\dagger}\hat{\tau}b_{l'})\right]\ .\end{aligned} \tag{15}$$

Here we have a fixed Cu—O—Cu bond $\langle ili'\rangle$, and l' is the only O-site index summed over. The subscripts on the sums merely show where the l' sites are located with respect to i and i'. For example, if the summation index is $\langle l'ili'\rangle$, we sum over the three O sites l' that are adjacent to Cu site i, and that are distinct from a fixed O site l, which is located between i and i'.

Whereas before only the J_2 term was present as a

source driving the large-scale Cu spin distortions, there are now hopping contributions to the current. However, we exclude the last line from what follows, since it represents the O spin transport due to the noninteracting hole motion.

It is of some interest to define a quantum operator whose expectation value gives the measure of the AF dipole moment directly. If we are interested in primarily the bond spin current, then a reasonable definition is [cf. Eq. (9)]

$$\mathbf{P}_a = \frac{1}{2J_1} \frac{\langle \{\hat{\mathbf{n}}_l, \mathbf{J}_{ii'}\} \rangle}{\langle \hat{\mathbf{n}}_l \rangle} \Bigg|_{l=i+\hat{\mathbf{a}}/2} , \tag{16}$$

where $\mathbf{J}$ is given in Eq. (15) with the $(t_a - t_b)$ term dropped, $\hat{\mathbf{n}}_l$ is the operator for the O density on site l, and $l=i+\hat{\mathbf{a}}/2$ is the O site lying between (i,i'). The operator in Eq. (16) is a vector in spin space but has also a spatial index, x or y, from the two possible bonds that the O hole can occupy. For example, $(i,i')=(1,2)$ for $\mu=x$ and (1,8) for $\mu=y$ (refer to Fig. 2). The factor of J_1 in the denominator makes the dimensions of Eq. (16) consistent with our earlier correlation functions.

Only the z-spin component of $\mathbf{P}_a$ is nonzero by the rotational symmetry around $\hat{\mathbf{z}}$. Furthermore, the a dependence is determined just by $\mathbf{k}$ in the manner expected by symmetry. At $\mathbf{k}=0$ and $(\pi,0)$, $\mathbf{P}$ vanishes; for $\mathbf{k}=(\pi/2,0)$, $P_{a=x} \neq 0$ while $P_{a=y}=0$. Finally, for $\mathbf{k}=(\pi/2,\pi/2)$, $P_{a=x}=P_{a=y}$. The last column of Table IV shows P_x for this value of $\mathbf{k}$ as a function of various parameters. In spite of the fact that we do not include $(\mathbf{S}_O \times \boldsymbol{\Omega})$ in the matrix element of Eq. (16), the dipole moment is independent of $t_a + t_b$ once it exceeds a fraction of J_1, provided J_2/J_1 is large enough, e.g., 3. Thus the dipole moment P_a can be saturated by J_2 for modest hopping, although it must vanish for $t_{a,b}=0$.

To conclude, we anticipate Sec. IV and give the semiclassical spin configuration (see Fig. 7) that reproduces the correlations among the total spin, O spin, and Cu spins. Of course, Fig. 7 must be understood as being averaged due to a rotation around $\hat{\mathbf{z}}$, and should be compared with Fig. 3 (quenched hole). The Cu spins are now predominantly in the x-y spin plane so that $\langle (\mathbf{S}_i \times \mathbf{S}_{i'})_z \rangle \neq 0$, but they are not coplanar and various products such as $\langle \mathbf{S}_O \cdot (\mathbf{S}_i \times \mathbf{S}_{i'}) \rangle \neq 0$. The local structure is still that of a spin polaron which is now oriented in the x-y plane to make $\langle S_O^z \rangle = 0$. Other insights into the $\mathbf{k}$ dependence of the quantum wave function can also be extracted semiclassically, and are contained in Sec. IV.

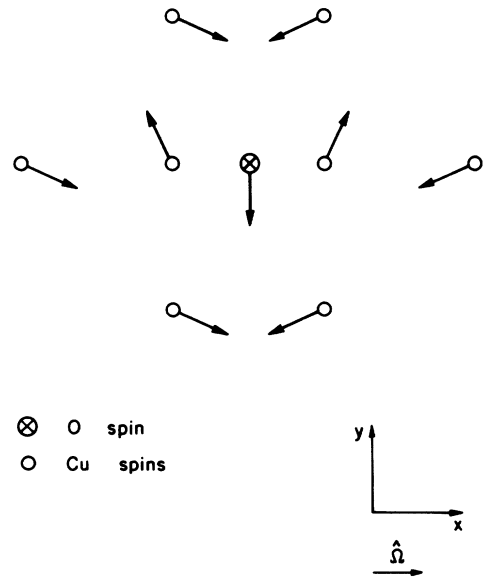

FIG. 7. Semiclassical spin configuration in the neighborhood of a mobile hole. Quantum mechanically, the total spin is to be thought of as directed out of the page, and the entire figure must thus be rotationally averaged around this direction in order to compare to the quantum cluster studies.

IV. SEMICLASSICAL APPROXIMATION

As previously mentioned, the quantum-mechanical wave functions for the 4×4 CuO_2 clusters are linear combinations of 48 620 states, and are difficult to interpret analytically. We attempt to gain some insight into the structure of the fully quantum-mechanical state by developing a semiclassical approximation. In this approximation we factorize the wave function into a product of spinors, and thus treat the exchange energy classically. Further, the hopping matrix elements between two such states may be evaluated exactly, and then the energy is minimized using the spinors as a set of variational parameters. This procedure supplements the quantum cluster studies in that much larger lattices may be studied. For 8×8 clusters, or 12×12, etc., more wave vectors along the magnetic Brillouin zone boundary, viz., $|k_x|+|k_y|=\pi$, may be studied than for the 4×4 cluster. The degeneracy (see Appendix A) of the $k=(\pi,0)$ and $(\pi/2,\pi/2)$ states is lifted. This approximation worked well in a study of the one-band model[22] in that a reasonable analytic understanding of the exact quantum cluster numerics was obtained.

A. Quenched hole

The spin of a hole occupying the jth site may be represented by a spinor,

$$\psi(j) = \begin{bmatrix} e^{-i\phi_j/2} & \cos(\theta_j/2) \\ e^{i\phi_j/2} & \sin(\theta_j/2) \end{bmatrix} . \tag{17a}$$

Then, the simplest wave function that may be formed is a product of such spinors, viz.,

$$|\Psi\rangle = \psi_0(R_0) \prod_j \psi(j - R_0) , \tag{17b}$$

where $\psi_0(R_0)$ is the spinor representing the O hole at site R_0, and the Cu sites are denoted by $\{j\}$. If $t_a=t_b=0$, the O hole is quenched, as in Sec. III b. Then, evaluation of $\langle \Psi | \hat{H}_{\text{eff}} | \Psi \rangle$ reduces the exchange interactions to a purely classical form, viz., $\mathbf{S}_j \cdot \mathbf{S}_{j'}$ becomes a scalar product of two classical Heisenberg spins.

The variational ground state is planar, and outside of

TABLE V. Bond spin currents for two semiclassical variational wave functions. The first column gives the values of $\langle(\mathbf{S}_2\times\mathbf{S}_3)_z\rangle$ for the ground state of Eq. (17b), arranged so that the spins are in the x-y plane. The second column gives the same correlation function for the ground state of Eq. (18a), which includes some of the quantum fluctuations of O hole's spin.

J_2/J_1	$\langle(\mathbf{S}_2\times\mathbf{S}_3)_z\rangle$ for Eq. (17b)	$\langle(\mathbf{S}_2\times\mathbf{S}_3)_z\rangle$ for Eq. (18a)
1	+0.065	+0.077
2	+0.107	+0.114
3	+0.132	+0.130
6	+0.166	+0.146
25	+0.198	+0.160

the core corresponds to a classical Néel configuration with a dipolar distortion, e.g., Eq. (9) with $f(r)\sim 1/r$. The long-range behavior of $f(r)$ follows from solving the Laplace equation for the angle defining the spin and matching onto the core region for small r. The dipole moment and hence the distortions depend on the ratio J_2/J_1. To compare quantitatively with Sec. III in Table V we show $\langle\mathbf{S}_2\times\mathbf{S}_3\rangle$ (cf. Fig. 2) for these wave functions. This correlation function is one of several possible measures of the dipole moment.

We also found from the classical variational solution that the O spin is perpendicular to the direction of the staggered magnetization (defined at $r\to\infty$), a feature that persists in all of our semiclassical studies. This can be understood in terms of the alignment of the staggered magnetization perpendicular to the "local field" produced by the O hole's spin.

The above discussion was purely classical, and to improve the solution near the hole, we include both O-spin states so as to more closely approximate the 3-spin polaron,

$$|\Psi_1\rangle=\alpha\psi_O^{\sigma}(R_O)\prod_j\psi^{\sigma}(j-R_O)+\beta\psi_O^{-\sigma}(R_O)\prod_j\psi^{-\sigma}(j-R_O)\ . \tag{18a}$$

The O spinor $\psi_O^{\sigma}(R_O)$ is chosen to have its spin σ in some direction, say, $+\hat{\mathbf{z}}$, and $\psi_O^{-\sigma}(R_O)$ is the time-reversed state $-\sigma$, say, $-\hat{\mathbf{z}}$. Thus, $\langle\psi_O^{\sigma}(R_O)|\psi_O^{-\sigma}(R_O)\rangle=0$ and the two spinor products in Eq. (18a) are orthogonal to one another. Consequently, all of the spins in $\psi^{\sigma}(j-R_O)$ and $\psi^{-\sigma}(j-R_O)$ may be taken to be completely independent of one another.

The utility of this form of a wave function is seen by consideration of a Cu-O-Cu cluster interacting according to Eq. (10a). The ground-state configuration is

$$|\Psi_1\rangle=\left[\frac{1}{2}\right]^{1/2}\left[\begin{bmatrix}\cos\frac{3\pi}{8}\\ \sin\frac{3\pi}{8}\end{bmatrix}_{\mathrm{Cu}(1)}\begin{bmatrix}1\\0\end{bmatrix}_O\begin{bmatrix}\cos\frac{3\pi}{8}\\ \sin\frac{3\pi}{8}\end{bmatrix}_{\mathrm{Cu}(2)}-\begin{bmatrix}\cos\frac{\pi}{8}\\ \sin\frac{\pi}{8}\end{bmatrix}_{\mathrm{Cu}(1)}\begin{bmatrix}0\\1\end{bmatrix}_O\begin{bmatrix}\cos\frac{\pi}{8}\\ \sin\frac{\pi}{8}\end{bmatrix}_{\mathrm{Cu}(2)}\right] \tag{18b}$$

and has an energy of $-(4)(0.96)J_2$. By comparison, the classical ground-state energy is $-2J_2$, while the exact result for Eq. (10b) is $-4J_2$.

We have numerically determined the ground state as a function of J_2/J_1 using Eq. (18a). The dipole moment and hence the spin distortions are changed by no more than 10% in comparison with Eqs. (17a) and (17b) (cf. Table V). However, the ground-state spin configuration is no longer planar close to the O hole. By that we mean that the spin vectors corresponding to individual spinors in Eq. (18a) are not coplanar, unlike in the case of Eq. (17b). Further, the expectation values of all the spin vectors in the system are still coplanar, resulting in the pattern of spins similar to that for Eq. (17b). In fact, the staggered magnetization, the dipole moment [cf. Eq. (9)], and $\langle\mathbf{S}_O\rangle$, are all mutually perpendicular. The quantization axis, $\hat{\mathbf{z}}$ in Eq. (18b), is parallel to the dipole moment. In Appendix B we show analytically that the distortion in the third dimension of the spinors in Eq. (18b) decays exponentially with a length scale given by $\sqrt{J_1/J_2}$. This length defines the characteristic size of the core region. Far from the O hole we still find a planar distortion that decays as r^{-1}.

B. Mobile hole

We now develop a simple variational approximation for the mobile hole. We incorporate a broken AF symmetry into our wave function, so that there are now four inequivalent O sites, denoted by μ, and two Cu spins in each magnetic unit cell. We introduce (see Fig. 8 for our labeling of the unit cell)

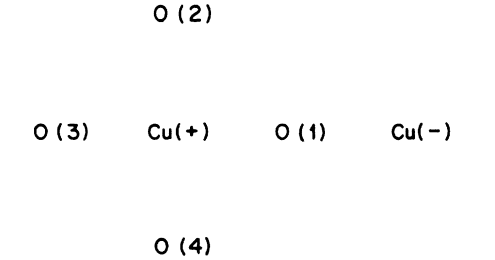

FIG. 8. Labeling of the magnetic unit cell used in Sec. IV. The four O sites, as well as the two Cu (up and down) sites are shown.

$$|\Psi\rangle=\sum_{\mu=1}^{4}|\Psi^{\mu}\rangle=\sum_{\mathbf{r}}\sum_{\mu=1}^{4}\gamma_{\mu}\psi_{\mathrm{O}}^{\mu}\prod_{i}\psi^{\mu}(i-\mathbf{r})e^{i\mathbf{k}\cdot\mathbf{r}}\ . \quad (19)$$

Here, the γ_μ are coefficients, the ψ_{O}^{μ} are the four O hole spinors, and $\psi^{\mu}(i-\mathbf{r})$ is the spinor for the Cu spin at site i, when the O hole is at site μ in the unit cell $\mathbf{r}$. Note that $|\gamma_\mu|^2$ is the probability for the O hole to be on site μ in a unit cell, if the spinors are all normalized.

1. Classical Néel limit

To gain some insight into the lowest band of states of this variational wave function, recall the results of Roth.[30] She essentially treats the wave function Eq. (19) with the constraint that the Cu spinors are frozen in a Néel configuration, say, $\mathbf{S}_i=\pm\frac{1}{2}\hat{\mathbf{z}}$. Under these assumptions no spin flip is possible, viz., there is no hopping process denoted by t_a+t_b (see Fig. 2), and the O hole's spin is "conserved." This implies at least doubly degenerate bands, and insures that we can label the band states by the O spin. The Cu and O spinors have thus been fixed. The only nontrivial variational parameters that are then left in Eq. (19) are the γ_μ, and we can then project Eq. (2) onto this subspace.

In terms of the two vectors

$$|1\rangle=\frac{1}{2}\begin{bmatrix}1\\1\\1\\1\end{bmatrix},\quad |k\rangle=\frac{1}{2}\begin{bmatrix}e^{ik_x}\\e^{ik_y}\\e^{-ik_x}\\e^{-ik_y}\end{bmatrix} \quad (20)$$

the new effective Hamiltonian can be exactly written as

$$\hat{H}_{\mathrm{eff,MF}}=-4t_a|1\uparrow\rangle\langle 1\uparrow|+4t_b|k\uparrow\rangle\langle k\uparrow| -4t_a|k\downarrow\rangle\langle k\downarrow|+4t_b|1\downarrow\rangle\langle 1\downarrow|\ . \quad (21)$$

The J_1 and J_2 terms have been dropped since they do not change with γ_μ or with the O spin's value.

In order to understand how Eq. (21) is obtained, consider $t_b=0$. Then, the only process allowed is the hopping of an O hole through a Cu site that has an antiparallel spin, with an amplitude $-t_a$. Choosing, say, the O spin to be up, the hole can only hop through the Cu spins in the Néel state that are down. Thus, the system entirely separates into cages[40,11] of four O sites around each down Cu spin. These cages do not communicate due to the absence of t_b, a hopping process through a parallel Cu spin. A single 4-site cage yields four solutions, three degenerate ones with energy t_a, and one with energy $-3t_a$. The wavefunction of the nondegenerate state is state $|1\rangle$ of Eq. (20). When all but one of the eigenstates of a given operator (in this case, the t_a part of the effective Hamiltonian) are degenerate, a single projection operator is sufficient to exactly represent it. Choosing the origin of energy as t_a, we obtain a $-4t_a$ term (with spin up) in Eq. (21). A similar calculation can be done with $t_a=0$, $t_b\neq 0$ (still for the O spin up). In this case, the noncommunicating cages are formed around the up Cu spins. However, the four sites in any of those cages all belong to different unit cells. Translating those four sites into a single unit cell, we obtain that $|k\rangle$ of Eq. (20) is now the appropriate nondegenerate state, which is used to represent the t_b term in Eq. (21). The same is done for the down O spin, and the exact representation [viz., Eq. (21)] of the mean-field effective Hamiltonian is thus obtained.

We stress again that O spin up and down states do not mix, as explained above. The O spin flip followed by the interchange $|k\rangle\leftrightarrow|1\rangle$ is a symmetry of this effective Hamiltonian. One can then see that in the four-dimensional γ_μ space (for a given O spin value) there are two eigenstates of Eq. (21) with energy zero, viz., the ones orthogonal to both $|1\rangle$ and $|k\rangle$. These are the nonbonding states. Two more eigenstates are obtained by solving a 2×2 problem in the space spanned by $|1\rangle$ and $|k\rangle$ [note that $\langle 1|k\rangle=\frac{1}{2}(\cos k_x+\cos k_y)$]. Solving this 2×2 problem yields[30]

$$E=2\{(t_b-t_a)\pm[(t_a+t_b)^2 -t_at_b(\cos k_x+\cos k_y)^2]^{1/2}\}\ , \quad (22a)$$

and the spin up and down eigenstates corresponding to the lower of these two energies are

$$\alpha|1\uparrow\rangle+\beta|k\uparrow\rangle\ ,\quad \alpha|k\downarrow\rangle+\beta|1\downarrow\rangle\ , \quad (22b)$$

where (up to a common normalization factor)

$$\alpha=(t_a+t_b)+[(t_a+t_b)^2-t_at_b(\cos k_x+\cos k_y)^2]^{1/2}\ ,\quad \beta=-t_b(\cos k_x+\cos k_y)\ . \quad (22c)$$

The band minimum in this calculation lies on the Brillouin zone boundary $|k_x|+|k_y|=\pi$, and the energy is degenerate along the zone boundary.

Especially simple answers are obtained in two special cases. On the zone boundary, i.e., at $|k_x|+|k_y|=\pi$, we have $\langle 1|k\rangle=0$, and the lowest energy states for both values of the O spin are simply $|1\uparrow\rangle$ and $|k\downarrow\rangle$, with $E=-4t_a$. At $\mathbf{k}=0$, we have $|1\rangle=|k\rangle$, so the space spanned by $|1\rangle$ and $|k\rangle$ is now only one dimensional. There are then three degenerate states with $E=0$, and one state with energy $E=-4t_a+4t_b$. If $t_a>t_b$, this is the minimum energy state at $\mathbf{k}=0$; otherwise there is a three-fold degeneracy (besides the spin degeneracy) of the minimum energy state at that point.

This simple calculation is unfortunately inadequate. Clearly we have to allow for Cu spin distortions. For example, this solution is misleading in that it predicts a bandwidth of order $-4\min(t_a,t_b)$, rather than of order J_1, as we found in Sec. III. However, the Roth solution will be useful in untangling the results of the variational calculation.

2. Exact numerical variational results

We next evaluated Eq. (2) for the trial wave function in Eq. (19), and have treated all of the spinors and the coefficients γ_μ as variational parameters to be minimized numerically. The resulting band is no longer degenerate

along the zone boundary, and the minimum is at $\mathbf{k}=(\pm\pi/2,\pm\pi/2)$. Ignoring an additive constant, this energy band can be approximately parametrized by the formula

$$E(\mathbf{k})=a(\cos k_x+\cos k_y)^2-2b(\sin^2 k_x+\sin^2 k_y)\ .$$

For an 8×8 lattice, using the values of parameters given in Eq. (7), we obtain

$$a\sim 0.30\ , \tag{23a}$$

$$b\sim 0.05\ . \tag{23b}$$

Note that the $(\sin^2 k_x+\sin^2 k_y)$ term breaks the degeneracy along the zone boundary. From this, we can estimate the transverse and normal masses at $\mathbf{k}=(\pm\pi/2,\pm\pi/2)$,

$$\begin{aligned} m_\perp &= \frac{1}{4(a+b)}\sim 0.72\ , \\ m_\parallel &= \frac{1}{4b}\sim 4.9\ . \end{aligned} \tag{24}$$

Thus the ratio of the two masses is $m_\parallel/m_\perp\sim 6.8$.

Next, we look at the O hole's spin and the four coefficients γ_μ. There is an O spin vector $\mathbf{S}_{\mathrm{O}}^\mu$ for each of the four O sites in a unit cell. In our numerical studies on the zone boundary, as well as at other k points close enough to it, we found that all four O spin vectors $\mathbf{S}_{\mathrm{O}}^\mu$ lie in the plane that is perpendicular to the asymptotic Néel order parameter $\hat{\mathbf{\Omega}}$ away from the hole. As we approach $\mathbf{k}=0$, the $\mathbf{S}_{\mathrm{O}}^\mu$ no longer lie in that plane, unless either $t_a=0$ or $t_b=0$. The exact location of the crossover region in $\mathbf{k}$ space, separating the states with a planar O spin configuration from nonplanar ones, depends on the exact values of the parameters. In general, the $\mathbf{S}_{\mathrm{O}}^\mu$ vectors point in different directions. Most interestingly, we obtained that on the zone boundary $\sum_{\mu=1}^4 \mathbf{S}_{\mathrm{O}}^\mu=0$. We also obtained that the four coefficients γ_μ have the same magnitude on the zone boundary. These two results mean that the expectation value of the O spin operator $\hat{\mathbf{S}}_{\mathrm{O}}$ vanishes on the zone boundary, viz., $\langle\Psi|\hat{\mathbf{S}}_{\mathrm{O}}|\Psi\rangle=0$. (The spin expectation value includes averaging over the four locations μ in the unit cell.) Besides the zone boundary, the coefficients have the same magnitude on the line(s) $|k_x|=|k_y|$, but are different elsewhere. We will see that many of these results can be derived from Roth wave functions.

Now consider the distortions of the AF Cu spin state. For each location μ of the O hole in a unit cell, there is a different Cu spin configuration $\mathbf{S}^\mu(i-\mathbf{r})$ [cf. Eq. (19)]. However, far away from the hole the Cu spin pattern has to be the same regardless of μ (see Appendix C for a proof). We thus find it useful to characterize the Cu spin distortion around the hole by taking the average of the four patterns,

$$\mathbf{S}(i-\mathbf{r})=\sum_\mu |\gamma_\mu|^2\mathbf{S}^\mu(i-\mathbf{r})\ .$$

Computing such quantities, we obtained that at $\mathbf{k}=(\pm\pi/2,\pm\pi/2)$ the nonuniform twist of the staggered order parameter has a dipolar symmetry. At $\mathbf{k}=(\pi,0)$, the distortion is quadrupolar in character.

These results agree qualitatively with the quantum cluster studies of Sec. III B. Thus it makes it all the more imperative to develop an analytical understanding of the variational solutions in order to have a simple way of understanding the qualitative behavior of the quantum states.

3. *Large-J_1 perturbation theory*

Our numerical results are predominantly for the physical limit $\{t_a,t_b,J_2\}\gg J_1$. The only apparently simple starting point for a perturbation theory is the Néel state, which requires that $J_1\gg\{t_a,t_b,J_2\}$. It is somewhat surprising, however, that the perturbation theory in this limit actually gives a rather accurate representation of many of the properties of the small-J_1 results, as we now demonstrate.

We develop a perturbation theory by starting with the Roth solutions [Eq. (22b)]. The Cu spins are exactly in the Néel state in the Roth wave functions, and there is a double degeneracy due to the O hole's spin. We know numerically, however, that this degeneracy is broken in our variational states. We thus choose a correct zeroth-order Roth solution, by combining the up and down O spin solutions at a given $\mathbf{k}$ in a way that assures that the O spin vectors $\mathbf{S}_{\mathrm{O}}^\mu$ lie in the x-y plane (assuming the Cu spins are in the $\pm\hat{\mathbf{z}}$ directions), as required by the exact numerical answer at and near the zone boundary. (The analogous construction for $\mathbf{k}$ near 0 is more complex and less interesting physically.)

The most general combination of the two degenerate Roth solutions with the desired properties is

$$|\Psi\rangle\sim(\alpha|1\uparrow\rangle+\beta|k\uparrow\rangle)+e^{i\phi}(\beta|1\downarrow\rangle+\alpha|k\downarrow\rangle)\ , \tag{25}$$

where $e^{i\phi}$ is a free phase, corresponding to rotations around the $\hat{\mathbf{\Omega}}$ direction, that can be set to 0. Note that the symmetry $|\uparrow\rangle\rightarrow|\downarrow\rangle$, $|1\rangle\rightarrow|k\rangle$, ensures that the spin is in the x,y plane and perpendicular to $\hat{\mathbf{\Omega}}$. This solution assumes a particularly simple form on the zone boundary, yielding

$$\begin{aligned} |\Psi\rangle &\sim |1\uparrow\rangle+|k\downarrow\rangle \\ &\sim \begin{bmatrix}1\\1\\1\\1\end{bmatrix}\otimes|\uparrow\rangle+\begin{bmatrix}e^{ik_x}\\e^{ik_y}\\e^{-ik_x}\\e^{-ik_y}\end{bmatrix}\otimes|\downarrow\rangle\ , \end{aligned} \tag{26a}$$

which implies for the four O spinors ψ_{O}^μ,

$$\begin{aligned} &\psi_{\mathrm{O}}^1\sim\begin{bmatrix}1\\e^{ik_x}\end{bmatrix},\ \psi_{\mathrm{O}}^2\sim\begin{bmatrix}1\\e^{ik_y}\end{bmatrix}, \\ &\psi_{\mathrm{O}}^3\sim\begin{bmatrix}1\\e^{-ik_x}\end{bmatrix},\ \psi_{\mathrm{O}}^4\sim\begin{bmatrix}1\\e^{-ik_y}\end{bmatrix}. \end{aligned} \tag{26b}$$

More compactly,

$$\psi_O^\mu = \begin{bmatrix} 1 \\ e^{i\mathbf{k}\cdot\hat{\mu}} \end{bmatrix},$$

where $\hat{\mu}$ is a unit vector ($\hat{\mu}=\pm\hat{\mathbf{x}},\pm\hat{\mathbf{y}}$) connecting a down Cu spin of the Néel state with one of the four neighboring O sites in the same unit cell (see Fig. 8). As one can see, each of the four corresponding O-spin vectors lies in the x-y plane making angles k_x, k_y, $-k_x$, $-k_y$ with respect to the x axis. Since $|k_x|+|k_y|=\pi$ on the zone boundary, the sum $\sum_{\mu=1}^{4}\mathbf{S}_O^\mu=0$. Since the coefficients γ_μ can be seen to be equal in magnitude on the zone boundary, this implies that the expectation value of the O spin operator vanishes when averaged over the four O sites, viz., $\langle\Psi|\hat{\mathbf{S}}_O|\Psi\rangle=0$ on the zone boundary. This very important result is confirmed numerically in the full variational calculation, and we have seen in Sec. III B that this is also observed for the quantum cluster.

For other points in $\mathbf{k}$ space away from the zone boundary we no longer have $\beta=0$ [cf. Eqs. (22b) and (22c)]. The directions of $\mathbf{S}_O^\mu$ now depend on the ratio α/β, which in turn depends on t_a/t_b. The corresponding $\mathbf{S}_O^\mu$ pattern is easy to obtain, and we do not write down the corresponding formulas. We note that the result agrees approximately with the angles between various $\mathbf{S}_O^\mu$ in the full numerical calculation with parameters given in Eq. (7).

The next issue to address is the Cu spin distortion. In the case when the Cu-Cu exchange interaction J_1 is the largest energy in the problem, the Cu spin state in our variational wave function is going to be nearly Néel. That makes it reasonable to start with the Roth solutions given above, and try to generate Cu spin distortions perturbatively.

Firstly, we modify the Roth solution by allowing for the distortions of the two Cu spins adjacent to the O hole in each of the four components of the wave function given in Eq. (19), while keeping Eq. (26b) values for O spinors and the coefficients γ_μ. The Cu spinors next to the O hole become

$$\begin{bmatrix} 0 \\ 1 \end{bmatrix} \rightarrow \frac{1}{(1+|\epsilon^\mu|^2)^{1/2}} \begin{bmatrix} \epsilon^\mu \\ 1 \end{bmatrix}, \quad \begin{bmatrix} 1 \\ 0 \end{bmatrix} \rightarrow \frac{1}{(1+|\rho^\mu|^2)^{1/2}} \begin{bmatrix} 1 \\ \rho^\mu \end{bmatrix}. \tag{27a}$$

We expand changes in energy from the Roth solution due to hopping and Cu-O exchange to linear order in ϵ^μ, ρ^μ, and expand the Cu-Cu exchange energy to quadratic order. Minimizing the resulting expression when the hole is on site μ, for the nearest-neighbor Cu spinors we obtain

$$\begin{bmatrix} \epsilon^\mu \\ 1 \end{bmatrix} = \begin{bmatrix} -qe^{-i\mathbf{k}\cdot\hat{\mu}} \\ 1 \end{bmatrix}, \quad \begin{bmatrix} 1 \\ \rho^\mu \end{bmatrix} = \begin{bmatrix} 1 \\ -qe^{i\mathbf{k}\cdot\hat{\mu}} \end{bmatrix}, \tag{27b}$$

where $q=\frac{1}{6}[(\frac{3}{2})(t_a+t_b)+J_2]/J_1$. Recalling that the corresponding O spinor was

$$\frac{1}{\sqrt{2}} \begin{bmatrix} 1 \\ e^{i\mathbf{k}\cdot\hat{\mu}} \end{bmatrix},$$

we see that the two Cu spins are tilted in a direction that is opposite to the O spin located between them. (This is because direct Cu-O exchange J_2, as well as hopping with exchange (t_a+t_b) are antiferromagnetic exchange processes.) Qualitatively similar distortions of these nearest-neighbor Cu spins are found in the exact wave function. This simple calculation is, however, not sufficient to break the degeneracy along the zone boundary.

We are interested in the distortions of all of the Cu spins, especially in the asymptotic region away from the O hole. It is quite hard to extend the above analytical method to other Cu spins, and still obtain a tractable calculation. Thus we resort to describing the Cu spins away from the hole by four continuous vector fields, one for each of the four components of Eq. (19), and then derive a system of four coupled differential equations for those fields. Then we study the far-field behavior of the solutions. These four fields are defined by the following continuum limit:

$$(-1)^j\mathbf{S}_j^\mu \rightarrow \mathbf{\Omega}^\mu(r) . \tag{28}$$

First, we expect that far enough from the hole the Cu-spin configuration $\mathbf{\Omega}^\mu(r)$ is independent of the hole location in a unit cell, i.e., $\mathbf{\Omega}^\mu(r)=\mathbf{\Omega}(r)$ for all μ. An ordered Néel Cu spin configuration is characterized by $\mathbf{\Omega}^\mu(r)$ being a constant vector field, say, $\mathbf{\Omega}(r)=\hat{\mathbf{z}}$. The distortions from the Néel state are then characterized by $\delta\mathbf{\Omega}(r)=\mathbf{\Omega}(r)-\hat{\mathbf{z}}$. We show that for small deviations from Néel order, a condition always fulfilled far enough from the hole, this field obeys the two-dimensional Laplace equation. The leading term in the expansion of $\delta\mathbf{\Omega}(r)$ is a dipolar term, which can be generally represented as

$$\delta\mathbf{\Omega} \sim \frac{\mathbf{p}\cdot\hat{\mathbf{r}}}{r}\mathbf{S}_\Omega , \tag{29}$$

where $\mathbf{p}$ and $\mathbf{S}_\Omega$ are vectors in real and spin space, respectively, defined in Appendix C.

We show in Appendix C that the Cu spin pattern away from the hole contains such a dipolar distortion, with $\mathbf{p}\sim(\sin k_x,\sin k_y)$, when $\mathbf{k}$ is on or near the zone boundary. Note that $|\sin k_x|=|\sin k_y|$ on the zone boundary, and thus the dipole moment is maximized at $\mathbf{k}=(\pm\pi/2,\pm\pi/2)$, and vanishes at $\mathbf{k}=(\pi,0)$.

In Appendix C, we also derive the contribution to the total energy due to the Cu spin distortion in the asymptotic region. It generates a term $-2b(\sin^2 k_x+\sin^2 k_y)$ in the energy, and b varies as $b\sim J_1$ when $J_1 \ll (t_a+t_b)$, and as $b\sim(t_a+t_b)^2/J_1$ when $J_1 \gg (t_a+t_b)$. One must qualify this result in that while this calculation serves to motivate this particular term which breaks the symmetry along the zone boundary, we cannot be sure from this crude calculation alone that the core region's contribution to the coefficient of such a term may not be of the opposite sign.

V. DIRECT OXYGEN HOPPING t_{pp}

It has recently been suggested that the magnitude of the direct O $2p\sigma$-$2p\sigma$ hopping frequency (to be denoted by t_{pp}) is not small,[41] and thus could be an important

feature of the doped CuO_2 system. Here we examine this possibility.

In Fig. 9 we have shown our choice of the $3d_{x^2-y^2}$ and $2p\sigma_{x(y)}$ phases. The sign of the t_{pd} overlap is unimportant since (i) after a transformation,[15] all such overlaps are of the same sign, and (ii) in our formulation of the effective Hamiltonian [Eq. (2)] all energies are of order t_{pd}^2 or t_{pd}^4. The situation for the t_{pp} overlaps is quite different. If we assume that the sign of the t_{pp} overlap shown in Fig. 9 (viz., between the O orbitals located at $\frac{1}{2}\hat{x}$ and $\frac{1}{2}\hat{y}$) is negative, then after the transformation mentioned above[15] all t_{pp} overlaps are of the same sign, and will be negative. Thus, we append the effective Hamiltonian [Eq. (2)] with

$$\hat{H}' = -|t_{pp}| \sum_{\sigma,\langle l,l'\rangle} (b_{l\sigma}^{\dagger} b_{l'\sigma} + \text{H.c.}) , \tag{30}$$

where $\langle l,l' \rangle$ denotes the four (direct) neighboring O sites of each O site. Present estimates[41] suggest that $|t_{pp}| \approx 0.7$ eV.

The simplest way of realizing the possible importance of this effect is by repeating the mean-field calculation that was given by Roth[30] including t_{pp}, viz., freeze the Cu spins in a classical Néel configuration, and then allow for a hole to hop, i.e., including only $-t_a$, t_b, and $-|t_{pp}|$ processes. The four energy bands that result are shown in Fig. 10, where $t_a = 0.46$, $t_b = 0.68$, and $|t_{pp}| = 0.7$ eV have been used. Note that $\mathbf{k} = (\pi/2, \pi/2)$ is now the minimum energy state, in contrast to the degenerate magnetic zone boundary minimum found for $|t_{pp}| = 0$. However, one may show that for $|t_{pp}| = 2t_b$, for t_a being arbitrary, the ground state is degenerate and corresponds to $|k_x| = |k_y|$. If $|t_{pp}| > 2t_b$, $\mathbf{k} = 0$ becomes the ground state. Now recall that the arguments presented in Sec. III for the existence of an AF dipole moment in the ground state of a single hole depended on the minimum energy state being at $\mathbf{k} = (\pi/2, \pi/2)$. If the t_{pp} hopping process does produce such a ground state, clearly it can have a very important effect.

Therefore, we have redone our quantum cluster studies

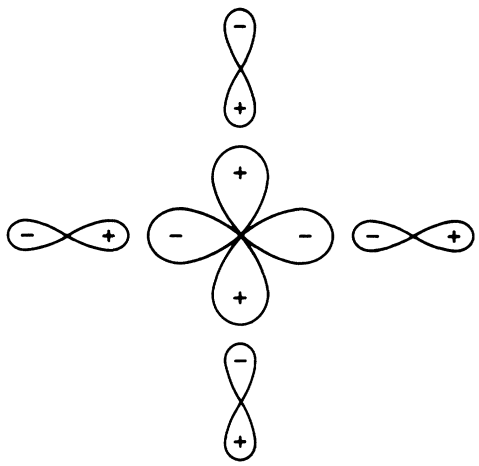

FIG. 9. p and d orbital phases adopted in Sec. V.

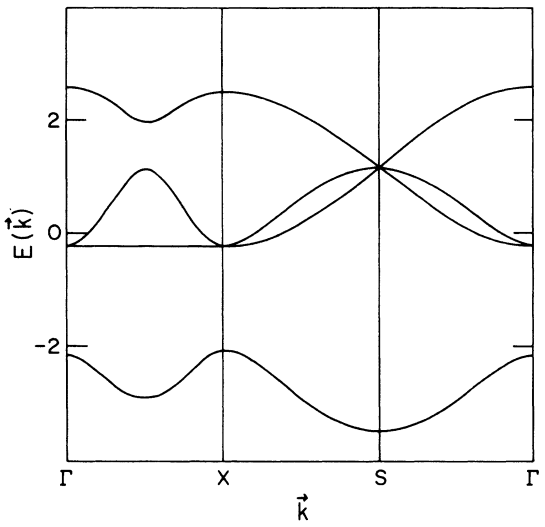

FIG. 10. Mean-field band structure for the parameters given in Eq. (7), including $t_{pp} = -0.7$ eV. The special points are Γ: $\mathbf{k} = 0$, X: $\mathbf{k} = (\pi, 0)$, and S: $\mathbf{k} = (\pi/2, \pi/2)$.

of Sec. III for the parameters given in Eq. (7) with the additional $\hat{H}'$ processes. When one includes the t_{pp} hopping, the arguments given in Appendix A are no longer correct, i.e., the $\mathbf{k} = (\pi, 0)$ and $\mathbf{k} = (\pi/2, \pi/2)$ states are nondegenerate, in general. We find that the ground state still corresponds to a $S = \frac{1}{2}$ state, with momentum $\mathbf{k} = (\pi/2, \pi/2)$, and

$$\left| E\left[\mathbf{k} = \left(\frac{\pi}{2}, \frac{\pi}{2}\right)\right] - E(\mathbf{k} = (\pi, 0)) \right| \approx 0.3 \text{ eV} ,$$

$$\left| E\left[\mathbf{k} = \left(\frac{\pi}{2}, \frac{\pi}{2}\right)\right] - E(\mathbf{k} = 0) \right| \approx 1 \text{ eV} .$$

Further, if we denote the minimum energy states determined for $t_{pp} = 0$ by $|\Psi_{\mathbf{k}}^0\rangle$, to better than one percent at all $\mathbf{k}$, we find that

$$E(\mathbf{k}) = \langle \Psi_{\mathbf{k}}^0 | (\hat{H} + \hat{H}') | \Psi_{\mathbf{k}}^0 \rangle , \tag{31}$$

i.e., one simply adds the $\hat{H}'$ energy, evaluated with respect to the $t_{pp} = 0$ ground-state wave function, which suggests that the effect is perturbative. The wave function is only weakly affected: Evaluating the various

TABLE VI. Minimum energies, in eV, for different wave vectors, of the quantum cluster when Eq. (30) is appended to our effective Hamiltonian for the standard parameters of Eq. (7).

t_{pp}	$E(\mathbf{k}=0)$	$E[\mathbf{k}=(\pi,0)]$	$E[\mathbf{k}=(\pi/2,\pi/2)]$
0.0	−16.268	−17.246	−17.246
−0.7	−17.936	−18.707	−18.941
−1.4	−19.96	−20.43	−20.85
−2.1	−22.06	−22.33	−22.79
−2.8	−24.39	−24.38	−24.83
−3.5	−26.81	−26.54	−26.97

TABLE VII. Expectation value of the O hole's spin as a function of t_{pp} for the standard parameters of Eq. (7).

t_{pp}	$\langle S_O^z \rangle$
0	±0.001
−0.7	−0.005
−1.4	−0.010
−2.1	−0.023
−2.8	−0.035
−3.5	−0.049

correlation functions discussed in Sec. III, we find that to within a few percent they do not change. For example, the dipole moment is unaffected by this value of t_{pp}.

Because of some uncertainty in the magnitude of t_{pp}, we have also produced minimum energy wave functions for larger values of this hopping frequency. The energies of the three aforementioned states are shown in Table VI. It is seen that even for five times the anticipated value (−3.5 eV) the minimum energy state still corresponds to $\mathbf{k}=(\pi/2,\pi/2)$. The principal effect of increasing the direct O hopping is the shift of $k=0$ energy downward relative to the zone boundary. Asymptotically for large $t_{pp}/(t_a+t_b)$ one expects the band minimum at the zone center, and the bandwidth scaling with t_{pp}.

From the set of $\mathbf{k}=(\pi/2,\pi/2)$ ground-state wave functions for each value of t_{pp} we have also calculated the expectation value of S_O^z. Our results are shown in Table VII. Clearly, as t_{pp} increases the O hole's spin deviates strongly from zero, thus raising a question about the adequacy, in this case, of the Zhang-Rice reduction.[11] This behavior has also been found by Schuttler *et al.*[17]

VI. CONCLUSIONS

Here we shall summarize our present understanding of the O hole ground state in the two-band model, and consider it in comparison with the t-J model to the extent possible. Indeed, taking into account that the two-band model has many more parameters, the similarity of the key results for the two models (in the physically interesting parameter range) is quite striking.

First, in both cases the bottom of the vacancy band is found at the face centers of the magnetic Brillouin zone and the bandwidth appears to scale with J (or J_1) in the large t/J [or $(t_a+t_b)/J_1$] limit. There is a difference, however, in that in the two-band model the hole bandwidth is finite already in the Ising limit,[30] with the energy minimum degenerate along the zone boundary (for $t_{pp}=0$), while for the t-J model in the corresponding limit the bandwidth is essentially zero.[35] The finite bandwidth in the t-J model is due mostly to the spin-flip process needed to relax the "string" of overturned spins left in the wake of the hopping hole. The physical reason behind the scaling of the bandwidth with J is likely to be the same for both models: In the large t/J limit there is a large distortion of the spin background near the hole (created by its virtual excursions) which can only drift coherently at the rate determined by J. Finally, the exact location of the energy minimum along the zone face, in general, is a difficult question to answer using small cluster calculations, because of the scarcity of Brillouin zone points available, and accidental symmetries (see Appendix A). For the t-J model the zone-face-center location of the minimum (at least for $t/J<10$) was obtained by studying the 18-site cluster. For the two-band model, it turns out that the inclusion of the direct O-O hopping lifts the accidental degeneracy of the 16-site cluster and places the band minimum unambiguously at the zone-face center. (This conclusion is consistent with the result of Shiba and Ogata[29] obtained for the smaller cluster.) We note that when the direct hopping rate becomes a few times larger than Cu-O hopping, the bottom of the hole band shifts back to $\mathbf{k}=0$. The considerable anisotropy of the mass appears to be quite sensitive to t_{pp}.

Another common property of the two models is the appearance of the dipolar distortion of the spin background. For the t-J model this dipole moment is due entirely to the hopping of the hole. For the two-band model the physics is somewhat more intricate with both Cu-O exchange and hopping contributing, apparently without significant competition. In essence, the effect is due to the appearance of the 3-spin polaron structure on the vacant bond. This local configuration of spins for a localized hole would be forced by Cu-O exchange,[15,18] but is also favored by the hopping which is facilitated by the overlap of the two neighboring copper spins.[15,22] Hence, provided $(t_a+t_b)/J_1$ is large, the 3-spin polaron has appreciable weight even if J_2 is zero. Semiclassical ideas then imply that there will be a long-range dipole distortion comoving with the hole. The spatial direction of the AF dipole moment that can be naturally associated with the hole is determined by the hole wave number. It follows by symmetry that the magnitude of the moment is maximal at the zone-face centers and vanishes at the center and the corners of the zone. We found that the moment can be saturated by both large J_2/J_1 and $(t_a+t_b)/J_1$. The spin direction of the AF dipole moment is determined by the spin of the vacancy state and in the semiclassical sense is perpendicular to both the O hole spin and the direction of the staggered magnetization.

A similar picture[19,22] emerged for the t-J model, although it was less straightforward, due to the absence of a locally defined hole spin. The dipole direction and the staggered magnetization were interpreted together as defining an SU(2) order parameter, and hence a triad of vectors. These operators were conjugate, in the quantum sense, to the magnetization, precisely as occurs in the nonlinear σ model, except that now rotations about $\boldsymbol{\Omega}$ act on the dipole direction and are physical. The semiclassical interpretation of these vectors is thus identical to that given for the two-band model.

A most obvious superficial distinction between the one and two-band models is the presence of the $\frac{1}{2}$ spin on the O hole site. However, the sharp distinction disappears for the hole ground state. Clearly, for both models the ground state on the lattice with an even number of Cu sites has the total spin $\frac{1}{2}$. The vacancy in the t-J model appears to acquire spin from the existence, in the presence of AF order, of two inequivalent sites per unit cell: Specifying the sublattice of the vacancy fixes the spin (in

the semiclassical sense) provided that the local direction of the staggered magnetization is specified. On the other hand, for the two-band model we found the O hole spin to be quenched (a similar observation was made by Reiter[31] and Schuttler and Fedro[17]), i.e., $\langle S_O^z \rangle = 0$, with the z component of magnetization taken up by the Cu spins. This can be understood as the tendency of the hopping to mix equally the states with opposite O spin in the unit cell doubled by the presence of AF order (the hole spin also tends to be perpendicular to the staggered magnetization). Finally, we note that the issue of the hole spin is quite important for understanding NMR experiments.[42]

We have seen that the long-wavelength properties and $E(\mathbf{k})$ in the Brillouin zone for the one- and two-band models are qualitatively similar. However, Zhang and Rice have suggested[11] that in a certain parameter range the two models are equivalent on the operator level. This being a rather strong statement, we have examined the local spin structure by projecting the exact ground state onto several reduced Hilbert spaces, the CuO_4 cluster of Zhang and Rice, and the Cu-O-Cu configuration proposed by Emery and Reiter.[15] However, in the former case we are only using the localized, nonorthogonal singlet structure, not the delocalized, orthogonal Wannier state structure which appears in the effective t-J model proposed by Zhang and Rice. Our numbers, in Table III, are suggestive of a very complicated fluctuating core region surrounding the O hole, one in which both the singlet and 3-spin polaron approximate a quasiparticle, but certainly in no fashion give credence to the concept of a strongly localized entity whose quantum spin fluctuations are unimportant. Furthermore, one might expect that the structure of the singlet quasiparticle, if identified, would depend nontrivially on the wave number. Unfortunately at this stage our study does not reach any firm conclusions on the issue.

An intrinsic limitation of the small cluster study, of course, are the finite-size effects, which limit the reliability of the estimates of mass anisotropy and, even more seriously, makes one worry about the results for larger values of the hopping to exchange ratio. The potential problem arises from the large size of the "core" region in that limit. In the case of the t-J model rather dramatic finite-size effects appeared for $t/J > 5$.

Finally, insight into the ground state of the O hole is a prerequisite for understanding experiments on doped CuO materials. Apart from the obvious importance of the hole band structure, the issue of O hole spin is relevant for interpreting the NMR (Ref. 42) measurements, while the presence of the long-range distortion of the staggered magnetization due the hole may explain the strong effect of the doping on the AF order.[18,22,43]

ACKNOWLEDGMENTS

The authors take pleasure in acknowledging stimulating discussions with Vinay Ambegaokar, Nick Bonesteel, Veit Elser, Vic Emery, and Andy Millis. One of us (D.M.F.) thanks AT&T Bell Laboratories for financial support. One of us (R.J.G.) acknowledges support from the National Sciences and Engineering Research Council of Canada (NSERC). One of us (E.D.S.) acknowledges support from the Guggenheim foundation as well as the hospitality of AT&T Bell Laboratories. This work was supported in part by the National Science Foundation (NSF) under Grant No. DMR8314625 and the U.S. Department of Energy under Grant No. DEAC0283ER13044.

APPENDIX A

The $\mathbf{k}=(\pi,0)$ and $\mathbf{k}=(\pi/2,\pi/2)$ states are degenerate in a 4×4 cluster with periodic boundary conditions due to an accidental symmetry which is present for both the one-[21] and two-band models (the latter only when the t_{pp} hopping is omitted). For a one-band model cluster, the simplest demonstration of the degeneracy is as follows. Consider the labeling of the Cu sites shown in Fig. 2, and suppose that an extra hole resides on site 7. At $\mathbf{k}=(\pi/2,\pi/2)$, when this hole hops to one of the four neighboring sites, the following phase factors arise: $7\rightarrow10$, $e^{i\mathbf{k}\cdot\mathbf{r}}=i$; $7\rightarrow6$, $e^{i\mathbf{k}\cdot\mathbf{r}}=i$; $7\rightarrow2$, $e^{i\mathbf{k}\cdot\mathbf{r}}=-i$; $7\rightarrow8$, $e^{i\mathbf{k}\cdot\mathbf{r}}=-i$. Now consider the "checkerboard rotation" of the cluster shown below,

$$\begin{array}{cccc} 16 & 15 & 14 & 13 \\ 9 & 10 & 11 & 12 \\ 8 & 7 & 6 & 5 \\ 1 & 2 & 3 & 4 \end{array} \rightarrow \begin{array}{cccc} 9 & 16 & 13 & 12 \\ 10 & 15 & 14 & 11 \\ 7 & 2 & 3 & 6 \\ 8 & 1 & 4 & 5 \end{array} . \tag{A1}$$

Note that every site in the transformed cluster has near neighbors that are identical to those in the original cluster (recall our use of periodic boundary conditions). For the same hole originally residing at site 7, and for $\mathbf{k}=(\pi,0)$, the phases corresponding to the hole's motion are $7\rightarrow10$, $e^{i\mathbf{k}\cdot\mathbf{r}}=-1$; $7\rightarrow6$, $e^{i\mathbf{k}\cdot\mathbf{r}}=-1$; $7\rightarrow2$, $e^{i\mathbf{k}\cdot\mathbf{r}}=+1$; $7\rightarrow8$, $e^{i\mathbf{k}\cdot\mathbf{r}}=+1$. Thus, apart from an unimportant overall phase of $(-i)$, these are identical to the $\mathbf{k}=(\pi/2,\pi/2)$ phase factors for the untransformed cluster, necessarily leading to the degeneracy of these states for this cluster.

The operation shown in Eq. (A1), to be denoted by C, is also a symmetry of the two-band Hamiltonian of Eq. (2), if we extend the definition of C to include the O holes. The hole location is determined by two of the Cu sites surrounding it. These two Cu sites will remain neighbors under C, and the bond now connecting them is where the transformed hole location is. In the two-band case the hole can hop to any of the six bonds which include the two Cu sites surrounding the occupied bond. After C is applied, the hole can still hop to any of those bonds, since these bonds are now connected to the two transformed Cu sites, and these two Cu sites are still neighbors. The t_{pp} hopping term [see Eq. (30)], does not, however, obey this symmetry, since the four Cu sites accessible to a given hole location in the untransformed cluster are no longer all accessible in the transformed cluster. For example, for the hole initially on the (7,8) bond, the (9.8) bond is (is not) accessible via t_{pp} hopping processes before (after) C is applied [see Eq. (A1)].

It remains to be determined how the crystal momen-

tum transforms under C. Denote translations of the cluster by *two* sites as $T_{2\hat{x}}$, $T_{2\hat{y}}$, and the inversion operation as I (under the inversion, 1↔13, 4↔16, etc.). One may establish the following identity:

$$C^{-1}T_{2\hat{x}}C = IT_{2\hat{y}} \ . \tag{A2}$$

Now consider a wave function $|\Psi\rangle$ with $\mathbf{k}=(\pi,0)$. Then, using Eq. (A2),

$$T_{2\hat{x}}C|\Psi\rangle = CIT_{2\hat{y}}|\Psi\rangle = CI|\Psi\rangle \ . \tag{A3}$$

Under inversion $(\pi,0)\rightarrow(-\pi,0)$, which is the same $\mathbf{k}$ point. Hence, we must have $I|\Psi\rangle=\pm|\Psi\rangle$. If the sign here is negative, then Eq. (A3) means

$$T_{2\hat{x}}C|\Psi\rangle = -C|\Psi\rangle \tag{A4}$$

and similarly for $T_{2\hat{y}}C|\psi\rangle$. In this case, $C|\Psi\rangle$ can only be a linear combination of states with momenta $\mathbf{k}=(\pm\pi/2,\pm\pi/2)$.

We have no general proof that the parity of $\mathbf{k}=(\pi,0)$ state has to be negative, but then we do observe the degeneracy in energy of $\mathbf{k}=(\pi,0)$ and $\mathbf{k}=(\pm\pi/2,\pm\pi/2)$ states for the two-band model.

APPENDIX B

Here we consider a simple wave function that includes the quantum fluctuations of the O hole's spin, and then solve for the distortions of the AF Cu spin state present in the ground state. We begin with the wave function given in Eq. (18a), written in the convenient form

$$|\Psi\rangle = |\Psi^{\uparrow}\rangle + |\Psi^{\downarrow}\rangle = \alpha \begin{bmatrix} 1 \\ 0 \end{bmatrix}_{\mathrm{O}} \prod_j \psi^{\uparrow}(R_j) + \beta \begin{bmatrix} 0 \\ 1 \end{bmatrix}_{\mathrm{O}} \prod_j \psi^{\downarrow}(R_j) \ , \tag{B1}$$

where $\binom{1}{0}_{\mathrm{O}}$ and $\binom{0}{1}_{\mathrm{O}}$ are the O spinors. The $\uparrow,\downarrow$ superscripts of the Cu spinors $\psi(R_j)$ refer to the O hole's spin. The energy expectation value has two diagonal terms, viz., the spin-spin interaction energy of each of the two components of the wave function, as well as the off-diagonal spin exchange energy on the Cu—O bonds, the latter being modified by an infinite overlap product between the two components of $|\Psi\rangle$.

The solution in a small region next to the O hole can be found, e.g., numerically. To study the long-range behavior of the ground state, we write down those portions of the energy which depend on the Cu spins other than those neighboring the O spin,

$$\begin{aligned} \Delta E &= \frac{J_1}{2} \sum_{\langle ij \rangle} [\cos(\gamma_{ij}^{\uparrow}) + \cos(\gamma_{ij}^{\downarrow})] \\ &\quad - \lambda J_2 \prod_j{}' [\bar{\psi}^{\uparrow}(R_j)\psi^{\downarrow}(R_j)] \\ &= \frac{J_1}{2} \sum_{\langle ij \rangle} [\cos(\gamma_{ij}^{\uparrow}) + \cos(\gamma_{ij}^{\downarrow})] \\ &\quad - \lambda J_2 \prod_j{}' \cos\left[\frac{\kappa_j^{\uparrow\downarrow}}{2}\right] \ . \end{aligned} \tag{B2}$$

Here, $\gamma_{ij}^{\uparrow}(\gamma_{ij}^{\downarrow})$ are the angles between neighboring Cu spin vectors in $|\Psi^{\uparrow}\rangle(|\Psi^{\downarrow}\rangle)$, and $\kappa_j^{\uparrow\downarrow}$ is the angle between Cu spin vectors corresponding to $\psi^{\uparrow}(R_j)$ and $\psi^{\downarrow}(R_j)$. The constant $(-\lambda J_2)$ is an off-diagonal exchange energy on the Cu—O—Cu bonds, and it is modified due to the overlap product from the remaining Cu spins. For example, for the 3-spin polaron [see Eq. (18b)], $\lambda=(2\sqrt{2}+1)$. This value is appropriate in the $J_2 \gg J_1$ limit. For other values of J_1, the Cu-O-Cu spin structure is modified, but λ remains of order 1.

We are interested in the asymptotic region far from the O hole, viz., where $(-1)^j\mathbf{S}_j \rightarrow \frac{1}{2}\hat{\mathbf{y}}$ is very nearly the solution to the Cu spins in the ground state. The deviations of $(-1)^j\mathbf{S}_j$ from $\hat{\mathbf{y}}$ in the $|\Psi^{\uparrow}\rangle$ and $|\Psi_{\downarrow}\rangle$ components of $|\Psi\rangle$ are parametrized by $\delta\varphi_j^{\uparrow}$, $\delta\theta_j^{\uparrow}$, $\delta\varphi_j^{\downarrow}$, and $\delta\theta_j^{\downarrow}$ [see Eq. (17a)]. In the asymptotic region, i.e., far from the O hole, we expand Eq. (B2) to lowest order in these variables, and obtain the deviation of energy from the state where the Cu spins are in the exact Néel configuration,

$$\begin{aligned} \delta E &= \tfrac{1}{4}J_1 \sum_{\langle ij \rangle}{}' [(\delta\theta_i^{\uparrow} - \delta\theta_j^{\uparrow})^2 + (\delta\theta_i^{\downarrow} - \delta\theta_j^{\downarrow})^2 \\ &\quad + (\delta\varphi_i^{\uparrow} - \delta\varphi_j^{\uparrow})^2 + (\delta\varphi_i^{\downarrow} - \delta\varphi_j^{\downarrow})^2] \\ &\quad + \tfrac{1}{8}\lambda^* J_2 \sum_j [(\delta\theta_j^{\uparrow} - \delta\theta_j^{\downarrow})^2 + (\delta\varphi_j^{\uparrow} - \delta\varphi_j^{\downarrow})^2] \ . \end{aligned} \tag{B3}$$

[λ^* is obtained from λ as follows. We have expanded the infinite product, and for this expansion to be valid we have had to exclude the terms in the product which individually significantly deviate from 1. We thus include part of the infinite overlap product $\prod_j'(\bar{\psi}_j^{\uparrow}\psi_j^{\downarrow})$ from the strongly distorted spins in λ, viz., those spins close to the Cu—O—Cu bond, thus obtaining a renormalized λ^*.]

Minimizing this energy deviation, and utilizing the continuum limit, we obtain

$$-\nabla^2(\delta\theta^{\uparrow}) + \frac{1}{2}\left[\lambda^*\frac{J_2}{J_1}\right](\delta\theta^{\uparrow} - \delta\theta^{\downarrow}) = 0 \ , \tag{B4}$$

$$-\nabla^2(\delta\theta^{\downarrow}) + \frac{1}{2}\left[\lambda^*\frac{J_2}{J_1}\right](\delta\theta^{\downarrow} - \delta\theta^{\uparrow}) = 0 \ , \tag{B5}$$

as well as two similar equations for $\delta\varphi^{\uparrow}$, $\delta\varphi^{\downarrow}$.

From the semiclassical 3-spin polaron solution [see Eq. (18b)], we expect $\delta\theta_j^{\uparrow} = -\delta\theta_j^{\downarrow}$, $\delta\varphi_j^{\uparrow} = \delta\varphi_j^{\downarrow}$. Numerical solutions on finite lattices confirm this symmetry. Using this symmetry in Eqs. (B4) and (B5) we obtain

$$-\nabla^2(\delta\theta)+\left[\lambda^*\frac{J_2}{J_1}\right](\delta\theta)=0\ , \tag{B6}$$

$$\nabla^2(\delta\varphi)=0\ . \tag{B7}$$

Thus, $\delta\theta$ goes to zero as $e^{-r/l}$, with a characteristic decay length

$$l\sim\left[\frac{J_1}{\lambda^*J_2}\right]^{1/2}\ . \tag{B8}$$

However, $\delta\varphi$ is described by Laplace's equation, and thus beyond $r\sim\sqrt{J_1/\lambda^*J_2}$ we obtain an essentially planar configuration, and the distortions induced are long ranged and have a dipolar symmetry.

APPENDIX C

In Sec. IV C, in a perturbative calculation, we found how the two Cu spins next to the O hole become distorted from their Néel values [cf. Eq. (27)]. One can ask which long-ranged AF Cu spin distortions are driven by these nearest-neighbor distortions. As we know from our quenched hole studies, if we could somehow turn off the hopping terms while freezing the distorted nearest-neighbor Cu spins, long-ranged dipolar Cu spin distortions would have resulted in each of the four components of the wave function of Eq. (19), viz.,

$$\delta\mathbf{S}_j^\mu\sim(-1)^j\frac{(p\hat{\boldsymbol{\mu}})\cdot\hat{\mathbf{r}}}{r}\mathbf{S}_{\mathrm{O}}^\mu=(-1)^j\frac{\mathbf{p}_\mu\cdot\hat{\mathbf{r}}}{r}\mathbf{S}_{\mathrm{O}}^\mu\ , \tag{C1}$$

where $\mathbf{r}$ points from the O hole to the Cu site j, μ labels the four components of the wave function of Eq. (19), and S_{O}^μ are the oxygen spin vectors in each of the four components of the wave function [cf. Eq. (9) and the preceding paragraph; we use coordinate-dependent notation for the dipolar distortions in this appendix]. These distortions are strongly modified by the hopping. Hopping matrix elements in the infinite system involve infinite overlap products,

$$P^{\mu\mu'}=\prod_j{}'\cos\left[\frac{\kappa_j^{\mu\mu'}}{2}\right]\ , \tag{C2}$$

where $\kappa_j^{\mu\mu'}$ is an angle between spin vectors $\mathbf{S}_j^\mu$ and $\mathbf{S}_j^{\mu'}$ at site j in two different components of the wave function, and the prime on the product sign indicates that some of the Cu spins near to the O hole are excluded from the product. We claim that if the dipolar distortions in the $|\Psi^\mu\rangle$ and $|\Psi^{\mu'}\rangle$ components of the wave function $|\Psi\rangle=\sum_{\mu=1}^4|\Psi^\mu\rangle$ are different, the overlap $P^{\mu\mu'}$ is zero. To prove this expand,

$$\begin{aligned}P^{\mu\mu'}&\simeq\prod_j{}'\left[1-\tfrac{1}{8}(\kappa_j^{\mu\mu'})^2\right]\\&\simeq\exp\left[-\tfrac{1}{8}\sum_j{}'(\kappa_j^{\mu\mu'})^2\right]\\&\simeq\exp\left[-\tfrac{1}{2}\sum_j{}'(\delta\mathbf{S}_j^\mu-\delta\mathbf{S}_j^{\mu'})^2\right]\ .\end{aligned} \tag{C3}$$

If $\sum_j'(\delta\mathbf{S}_j^\mu-\delta\mathbf{S}_j^{\mu'})^2$ diverges, the infinite product will be zero. Define $\boldsymbol{\Omega}_j^\mu=(-1)^j\mathbf{S}_j^\mu$. Then, employing the continuum approximation,

$$\begin{aligned}\sum_j{}'(\delta\mathbf{S}_j^\mu-\delta\mathbf{S}_i^{\mu'})^2&\rightarrow\int d^2r[\delta\boldsymbol{\Omega}^\mu(r)-\delta\boldsymbol{\Omega}^{\mu'}(r)]^2\\&=\int r\,dr\,d\theta\frac{[(\mathbf{p}_\mu\cdot\hat{\mathbf{r}})\mathbf{S}_{\mathrm{O}}^\mu-(\mathbf{p}_{\mu'}\cdot\hat{\mathbf{r}})\mathbf{S}_{\mathrm{O}}^{\mu'}]^2}{r^2}\\&=\int\frac{dr}{r}\int d\theta[(\mathbf{p}_\mu\cdot\hat{\mathbf{r}})\mathbf{S}_{\mathrm{O}}^\mu-(\mathbf{p}_{\mu'}\cdot\hat{\mathbf{r}})S_{\mathrm{O}}^{\mu'}]^2\ .\end{aligned} \tag{C4}$$

While the integral $\int dr/r$ should be cut off at the lower limit, it still diverges at the upper limit. To avoid divergence, we have to have $\mathbf{p}_\mu=\mathbf{p}_{\mu'}$, $\mathbf{S}_{\mathrm{O}}^\mu\rightarrow\mathbf{S}_{\mathrm{O}}^{\mu'}$.

To avoid this "overlap catastrophe," the dipolar distortions have to be the same in all four components of the wave function, at least asymptotically. It is clear from the above, however, that the nearest-neighbor distortions in different $|\Psi^\mu\rangle$ attempt to create different dipole moments, and it is only hopping, acting through overlap integrals, that brings them into correspondence. We now analyze how the different dipolar distortions, driven within each $|\Psi^\mu\rangle$ component, approach a common solution.

Similar to the approach used in Appendix B, we assume that we somehow know the solution in a finite region around the O hole, either numerically or perturbatively. Let $\boldsymbol{\omega}^\mu(r)$ be the far-field solution that results from relaxing the Cu-Cu exchange alone, with the local solution [e.g., (27b)] frozen and used as a boundary condition, i.e., an equation similar in form to Eq. (C1). Also, let the hopping matrix elements (to be modified by overlap products) on this finite lattice be $H_{\mu\mu'}^{\mathrm{hop}}$. Then the energy functional in the $\boldsymbol{\Omega}^\mu(r)$ fields (to be varied outside that finite region) becomes

$$\begin{aligned}\Delta E=&\tfrac{1}{2}J_1\sum_\mu\int d^2r[\partial_i(\boldsymbol{\Omega}^\mu(r)-\boldsymbol{\omega}^\mu(r))]^2\\&+\sum_\mu\sum_{\mu'}H_{\mu\mu'}^{\mathrm{hop}}\exp\left[-\tfrac{1}{2}\int d^2r[\boldsymbol{\Omega}^\mu(r)-\boldsymbol{\Omega}^{\mu'}(r)]^2\right]\ .\end{aligned} \tag{C5}$$

Here, we have expanded the overlap product as above.

Upon expanding the exponential in Eq. (C5), the variation of ΔE with respect to $\boldsymbol{\Omega}^\mu(r)$ gives

$$-\nabla^2\boldsymbol{\Omega}^\mu-\sum_{\mu'}\frac{H_{\mu\mu'}^{\mathrm{hop}}}{J_1}(\boldsymbol{\Omega}^\mu-\boldsymbol{\Omega}^{\mu'})=0\ . \tag{C6}$$

Here we used the result that $\boldsymbol{\omega}^\mu(r)$ obeys the two-dimensional Laplace equation. Now define

$$\mathbf{g}(r)=\tfrac{1}{4}\sum_\mu\boldsymbol{\Omega}^\mu(r)\ . \tag{C7}$$

Summing over the four relations given by Eq. (C6), we obtain

$$\nabla^2\mathbf{g}(r)=0\ . \tag{C8}$$

Thus, the average Cu spin order parameter obeys the Laplace equation.

We now want to see how this averaged solution is ap-

proached by the individual $\Omega^{\mu}(r)$. While this step is inessential, to simplify further presentation, let $H^{\rm hop}_{\mu\mu'}=\text{const}=-\frac{1}{4}t$. Then, from Eq. (C6) we obtain

$$-\nabla^2\Omega^{\mu}+\frac{t}{J_1}[\Omega^{\mu}-\mathbf{g}(r)]=0 \ . \tag{C9}$$

Thus, all Ω^{μ} approach $\mathbf{g}(r)$ exponentially, with a characteristic length scale

$$l\sim\sqrt{J_1/t} \ . \tag{C10}$$

Except at special $\mathbf{k}$ points, $\mathbf{g}(r)$ is expected to have a dipolar term; it is, however, difficult to determine its specific functional form. In order to obtain a rough idea of what $\mathbf{g}(r)$ is in the remainder of the appendix we use a crude approximation and set all $\Omega^{\mu}(r)\equiv\mathbf{g}(r)$. Then the integral in the exponential in Eq. (C5) is zero, and

$$\Delta E=\tfrac{1}{2}J_1\sum_{\mu}\int d^2r[\partial_i(\mathbf{g}(r)-\omega^{\mu}(r))]^2+\text{const} \ . \tag{C11}$$

This is minimized when $\mathbf{g}(r)=\frac{1}{4}\sum_{\mu}\omega^{\mu}(r)$. Thus, in this rough approximation, the long-ranged dipolar distortion is just the average of those that would have occurred in the four components of $|\Psi\rangle$ if the hopping only affected the Cu spins next to the O hole. Since we obtained, under these conditions, $\omega^{\mu}(r)\sim[(\hat{\boldsymbol{\mu}}\cdot\hat{\mathbf{r}})/r]\mathbf{S}^{\mu}_{\rm O}$, we find

$$\mathbf{g}(r)\sim\tfrac{1}{4}\sum_{\mu}\frac{\hat{\boldsymbol{\mu}}\cdot\hat{\mathbf{r}}}{r}\mathbf{S}^{\mu}_{\rm O}$$
$$\sim\frac{1}{4}\left[\frac{\hat{\mathbf{x}}\cdot\hat{\mathbf{r}}}{r}(\mathbf{S}^1_{\rm O}-\mathbf{S}^3_{\rm O})+\frac{\hat{\mathbf{y}}\cdot\hat{\mathbf{r}}}{r}(\mathbf{S}^2_{\rm O}-\mathbf{S}^4_{\rm O})\right] . \tag{C12}$$

At $\mathbf{k}=(\pi,0)$, we had (cf. Sec. IV C) $\mathbf{S}^1_{\rm O}=\mathbf{S}^3_{\rm O}$ and $\mathbf{S}^2_{\rm O}=\mathbf{S}^4_{\rm O}$. Then $\mathbf{g}(r)=0$, and there are no long-ranged dipolar distortions. At other points on the zone boundary, we recall (cf. Sec. IV C) that $\mathbf{S}^1_{\rm O}-\mathbf{S}^3_{\rm O}=\sin k_x\,\hat{\mathbf{y}}$ and $\mathbf{S}^2_{\rm O}-\mathbf{S}^4_{\rm O}=\sin k_y\,\hat{\mathbf{y}}$, up to an overall rotation in spin space around $\hat{\mathbf{z}}$. So,

$$\mathbf{g}(r)\sim\frac{(\sin k_x\hat{\mathbf{x}}+\sin k_y\,\hat{\mathbf{y}})\cdot\hat{\mathbf{r}}}{r}\mathbf{S}_{\Omega} \ , \tag{C13}$$

where we replaced $\hat{\mathbf{y}}\rightarrow\mathbf{S}_{\Omega}$ to emphasize that this is a spin-space vector, of unit magnitude. The strength of dipole distortion is given by $(\sin k_x\hat{\mathbf{x}}+\sin k_y\,\hat{\mathbf{y}})$, which is maximized at $\mathbf{k}=(\pi/2,\pi/2)$, and vanishes at $\mathbf{k}=(\pi,0)$, as expected.

We now return to the expression (C11) for ΔE, drop the constant, and rewrite it as

$$\Delta E=2J_1\sum_i\int d^2r\left\{\left[\partial_i\left[\mathbf{g}-\tfrac{1}{4}\sum_{\mu}\omega^{\mu}(r)\right]\right]^2+\tfrac{1}{4}\sum_{\mu}[\partial_i\omega^{\mu}(r)]^2-\left[\tfrac{1}{4}\sum_{\mu}\partial_i\omega^{\mu}(r)\right]^2\right\} . \tag{C14}$$

This is minimized when $\mathbf{g}(r)=\frac{1}{4}\sum_{\mu}\omega^{\mu}(r)$ and equals

$$\Delta E=2J_1\int d^2r\left[\tfrac{1}{4}\sum_{\mu}[\partial_i\omega^{\mu}(r)]^2-[\partial_i\mathbf{g}(r)]^2\right] . \tag{C15}$$

Only the second term is $\mathbf{k}$ dependent, and we study its contribution to the energy. First, we note that this contribution is of the form

$$\delta E=-2b\,(\sin^2k_x+\sin^2k_y) \ , \tag{C16}$$

and we are interested in knowing the behavior of the coefficient b at various values of the parameters. Recall that $\mathbf{g}(r)$ is made up of the individual $\omega^{\mu}(r)$. The latter are just the long-ranged deviations from Néel order driven by the distortions of the Cu spins next to the O hole. As we saw in Sec. IV C, in the limit $\{t_a,t_b,J_2\ll J_1\}$, those Cu spins were tipped by an angle $\sim t_{ab}/J_1$. So, $\mathbf{g}(r)$ is also $\sim t_{ab}/J_1$, and thus we obtain $b\sim J_1(t_a/J_1)^2\sim(t_{ab})^2/J_1$. In the opposite limit, viz., $\{t_a,t_b,J_2\gg J_1\}$, the $\omega^{\mu}(r)$ saturate, and then the integral corresponding to the second term in Eq. (C15) is of order $O(1)$. Then we expect $b\sim J_1$.

*Current address: Institute for Theoretical Physics, University of California–Santa Barbara, Santa Barbara, California 93106.

†Permanent address: Queens University, Kingston, Ontario, K7L3NG, Canada.

[1]J. G. Bednorz and K. A. Müller, Z. Phys. B **64**, 189 (1986); M. K. Wu, J. R. Ashburn, C. J. Torng, P. H. Hor, R. L. Meng, L. Gao, Z. J. Huang, Y. Q. Wang, and C. W. Chu, Phys. Rev. Lett. **58**, 908 (1987).

[2]W. E. Pickett, Rev. Mod. Phys. **61**, 433 (1989); and references therein.

[3]P. W. Anderson, Science **235**, 1196 (1987).

[4]C. M. Varma, S. Schmitt-Rink, and. E. Abrahams, Solid State Commun. **62**, 681 (1987).

[5]V. J. Emery, Phys. Rev. Lett. **58**, 2794 (1987).

[6]D. Vaknin, S. K. Sinha, D. E. Moncton, D. C. Johnston, J. Newsam, S. R. Safinya, and H. King, Phys. Rev. Lett. **58**, 2802 (1987); J. M. Tranquada, D. E. Cox, W. Kunnmann, H. Moudden, G. Shirane, M. Suenaga, P. Zolliker, D. Vaknin, S. K. Sinha, M. S. Alvarez, A. J. Jacobson, and D. C. Johnston, *ibid.* **60**, 156 (1988).

[7]T. Freltoft, G. Shirane, S. Mitsuada, J. P. Remeika, and A. S. Cooper, Phys. Rev. Lett. **37**, 137 (1988).

[8]J. M. Tranquada, S. M. Heald, and A. R. Moodenbaugh, Phys. Rev. B **36**, 5263 (1987).

[9]P. W. Anderson, Phys. Rev. **115**, 2 (1959).

[10]N. Nücker, J. Fink, J. C. Fuggle, P. J. Durham, and W. M. Temmerman, Phys. Rev. B **37**, 5158 (1988); M. W. Shafer, T. Penney, and B. L. Olson, *ibid.* **36**, 4047 (1987).

[11]F. C. Zhang and T. M. Rice, Phys. Rev. B **37**, 3759 (1988).

[12]E. B. Stechel and D. R. Jennison, Phys. Rev. B **38**, 4632 (1988); **38**, 8873 (1988).

[13]M. Ogata and H. Shiba, J. Phys. Soc. Jpn. **57**, 3074 (1988).
[14]P. Prelovsek, Phys. Lett. A **126**, 287 (1988); J. Zaanen and A. M. Moles, Phys. Rev. B **37**, 9423 (1988).
[15]V. J. Emery and G. Reiter, Phys. Rev. B **38**, 4547 (1988).
[16]A. F. Barabanov, L. A. Maximov, and G. V. Uimin, Pis'ma Zh. Eksp. Teor. Fiz. **47**, 532 (1988) [JETP Lett. **47**, 622 (1988)].
[17]H.-B. Schüttler and A. J. Fedro, Bull. Am. Phys. Soc. **34**, 925 (1989).
[18]A. Aharony, R. J. Birgeneau, A. Congilio, M. A. Kastner, and H. E. Stanley, Phys. Rev. Lett. **60**, 1330 (1988).
[19]B. I. Shraiman and E. D. Siggia, Phys. Rev. Lett. **60**, 740 (1988).
[20]S. A. Trugman, Phys. Rev. B **37**, 1597 (1988).
[21]V. Elser, D. Huse, B. I. Shraiman, and E. D. Siggia, Phys. Rev. B (to be published).
[22]B. I. Shraiman and E. D. Siggia, Phys. Rev. Lett. **61**, 467 (1988).
[23]C. L. Kane, P. A. Lee, and N. Read, Phys. Rev. B **39**, 6880 (1989).
[24]Schmitt-Rink, C. M. Varma, and A. E. Ruckenstein, Phys. Rev. Lett. **60**, 2793 (1988).
[25]S. Sachdev, Phys. Rev. B **39**, 12 232 (1989).
[26]J. Bonca, P. Prelovsek, and I. Sega, Phys. Rev. B **39**, 7074 (1989).
[27]Y. Hasegawa and D. Poilblank, Phys. Rev. B **40**, 9044 (1989).
[28]E. Dagotto (unpublished).
[29]H. Shiba and M. Ogata, Tech. Rep. ISSP, Ser. A, 2103 (1989).
[30]L. M. Roth, Phys. Rev. Lett. **60**, 379 (1988).
[31]G. Reiter (unpublished).
[32]D. C. Mattis, C. Y. Pan, and H. Q. Lin, J. Phys. Condensed Matter **1**, 135 (1989).
[33]B. I. Shraiman and E. D. Siggia, Phys. Rev. Lett. **62**, 1564 (1989).
[34]M. Schluter, Int. J. Mod. Phys. B **2**, 1 (1988).
[35]W. A. Brinkman and T. M. Rice, Phys. Rev. B **2**, 1324 (1970).
[36]E. Lieb, T. Schultz, and D. Mattis, Ann. Phys. (N.Y.) **16**, 407 (1961).
[37]J. B. Torrance, Y. Nokura, A. I. Nazzal, A. Bezinge, T. C. Huang, and S. S. Parkin, Phys. Rev. Lett. **61**, 1127 (1988).
[38]This correlation function carries complementary information to $\langle \mathbf{S}_l \cdot \mathbf{S}_{l'} \rangle$ even though $(\mathbf{S}_l \cdot \mathbf{S}_{l'})^2 + (\mathbf{S}_l \times \mathbf{S}_{l'})^2 = \frac{9}{16}$. When the nonlinear σ model applies, $\langle \mathbf{S}_l \times \mathbf{S}_{l'} \rangle$ measures a twist of the order parameter while $\langle \mathbf{S}_l \cdot \mathbf{S}_{l'} \rangle$ largely measures the reduction in Ω due to quantum fluctuations.
[39]For a quenched hole, this scalar product is identical to that on a bond equal to $\langle \mathbf{S}_4 \cdot \mathbf{S}_1 \rangle$, due to an obvious symmetry, but on a 4×4 lattice with periodic boundary conditions it is also equal to $\langle \mathbf{S}_2 \cdot \mathbf{S}_7 \rangle = \langle \mathbf{S}_1 \cdot \mathbf{S}_8 \rangle = \langle \mathbf{S}_1 \cdot \mathbf{S}_{16} \rangle = \langle \mathbf{S}_2 \cdot \mathbf{S}_{15} \rangle$.
[40]J. E. Hirsch, Phys. Rev. Lett. **59**, 228 (1987).
[41]M. S. Hybertsen and M. Schluter, Bull. Am. Phys. Soc. **34**, 424 (1989).
[42]R. E. Walstedt, W. W. Warren, R. F. Bell, G. F. Brenert, G. P. Espinosa, R. J. Cava, L. F. Schneemeyer, and J. V. Wasczak, Phys. Rev. B **38**, 9299 (1988).
[43]R. J. Birgeneau, D. R. Gabbe, H. P. Jenssen, M. A. Kastner, P. J. Picone, T. R. Thurston, G. Shirane, Y. Endoh, M. Sato, K. Yamada, Y. Hidaka, M. Oda, Y. Enomoto, M. Suzuki, and T. Muarkami, Phys. Rev. B **38**, 6614 (1988); J. M. Tranquada, A. M. Moudden, A. I. Goldman, P. Zolliker, D. E. Cox, G. Shirane, S. K. Sinha, D. Vaknin, D. C. Johnston, M. S. Alvarez, A. J. Jacobson, J. T. Lewandowski, and J. M. Newsam, *ibid.* **38**, 2477 (1988).